CHAPTER

Nearly Free Electron Model

4

CHAPTER OUTLINE

Physics of Condensed Matter. DOI: 10.1016/B978-0-12-384954-0.00004-9

4.1 ELECTRONS IN A WEAK PERIODIC POTENTIAL

4.1.1 Introduction

In the nearly free electron approximation, it is assumed that there are no electron–electron or electron–phonon interactions. This means that a valence electron, stripped from its parent atom due to the attractive interaction of the neighboring positively charged ions, does not interact either with other electrons or with the vibrating motion of the ions at a finite temperature. However, unlike the free electron approximation, the electron is subjected to a weak periodic potential due to the background of symmetric array of positively charged ions in the crystal lattice. We will first show that this potential is periodic with the periodicity of a lattice vector.

As an example, we consider a two-dimensional rectangular lattice, as shown in Figure 4.1.

If $\mathbf{OO'} = \vec{R}_i$ and $\mathbf{OE} = \vec{r}$, the potential energy at the electron E (charge $-e$) due to the positively charged ions of the crystal lattice (one ion of charge ze is assumed to be located at each lattice site) is given by

$$V(\vec{r}) = \sum_i \frac{-ze^2}{|\vec{r} - \vec{R}_i|}. \tag{4.1}$$

Here, we have considered the fundamental principle of electrostatics that in a spherical charge distribution, the potential at a point outside the sphere is the same as that of the potential due to the net charge considered to be located at the center of the sphere.

If $\vec{r}$ is translated by a lattice vector $\vec{R}_j$, Eq. (4.1) can be written in the alternate form

$$V(\vec{r} + \vec{R}_j) = \sum_i \frac{-ze^2}{|\vec{r} - \vec{R}_i + \vec{R}_j|}. \tag{4.2}$$

One can write $\vec{R}_i - \vec{R}_j = \vec{R}_l$, in which case Eq. (4.2) can be written in the alternate form

$$V(\vec{r} + \vec{R}_j) = \sum_l \frac{-ze^2}{|\vec{r} - \vec{R}_l|}. \tag{4.3}$$

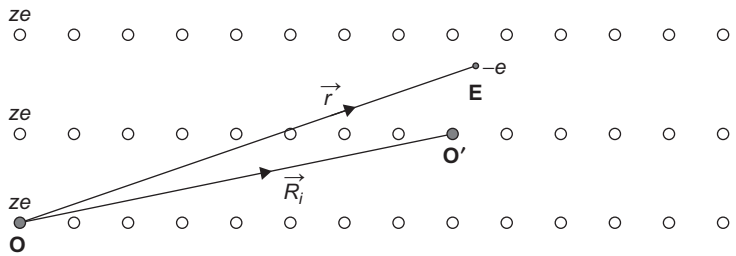

FIGURE 4.1

Two-dimensional rectangular lattice with **O** as the global origin and **O′** as the local origin of the unit cell within which the electron of charge $-e$ is located at **E**. The charge of each ion is ze.

Because the summation over both $\vec{R}_i$ and $\vec{R}_l$ spans the entire lattice vectors, we obtain from Eqs. (4.1) and (4.3)

$$V(\vec{r}) = V(\vec{r} + \vec{R}_j). \tag{4.4}$$

Eq. (4.4) clearly demonstrates that $V(\vec{r})$ is a periodic potential with the periodicity of a direct lattice vector. It may be noted that this proof was based on the simple assumption that an ion of charge ze is located at each lattice point. However, the proof can be generalized to an identical cluster of ions (a basis), located symmetrically around each lattice point.

4.1.2 Plane Wave Solutions

For simplicity, we consider a linear lattice of lattice constant a. Later, we will generalize our results to a three-dimensional lattice. From Eq. (4.4), the periodic potential in a one-dimensional lattice can be written as

$$V(x) = V(x + n\,a), \tag{4.5}$$

where n is an integer. If we express the periodic potential $V(x)$ as a Fourier series

$$V(x) = \sum_{q'} V(q') e^{iq'x}, \tag{4.6}$$

we obtain

$$V(x + na) = \sum_{q'} V(q') e^{iq'(x+na)}. \tag{4.7}$$

From Eqs. (4.5) through (4.7), it is easy to show that

$$\sum_{q'} V(q') e^{iq'x} = \sum_{q'} V(q') e^{iq'(x+na)}. \tag{4.8}$$

Eq. (4.8) has to be valid for each value of the integer n. This is possible only if

$$e^{iq'na} = 1, \tag{4.9}$$

for all values of n and q'. This condition is satisfied only when $q' = 2\pi m/a$, where m is any integer. This is precisely the definition of a reciprocal lattice vector K in one dimension and hence $q' = K$. The periodic potential $V(x)$ in Eq. (4.3) can therefore be expressed as

$$V(x) = \sum_{K} V(K) e^{iKx}. \tag{4.10}$$

The Schrodinger equation of the electron in a one-dimensional lattice is easily obtained,

$$\left(-\frac{\hbar^2}{2m}\frac{\partial^2}{\partial x^2} + \sum_{K} V(K) e^{iKx}\right)\psi(x) = E\psi(x), \tag{4.11}$$

where E is the energy eigenvalue and $\psi(x)$ is the wave function of the electron. The Born–von Karman boundary conditions imply that

$$\psi(x + Na) = \psi(x + L) = \psi(x). \tag{4.12}$$

$\psi(x)$ can also be expanded in terms of the plane waves, which are a complete set of functions,

$$\psi(x) = \sum_q a(q)e^{iqx}. \tag{4.13}$$

From Eqs. (4.11) and (4.13), we obtain

$$\sum_q \varepsilon_q^0 a(q)e^{iqx} + \sum_K \sum_q V(K)a(q)e^{i(q+K)x} = E\sum_q a(q)e^{iqx}, \tag{4.14}$$

where

$$\varepsilon_q^0 = \frac{\hbar^2 q^2}{2m}. \tag{4.15}$$

We assume that the one-dimensional crystal has a length L. Multiplying Eq. (4.14) by $e^{-iq'x}$ and integrating over x from 0 to L, we obtain

$$\sum_q \varepsilon_q^0 a(q)\int_0^L e^{i(q-q')x}dx + \sum_K \sum_q V(K)a(q)\int_0^L e^{i(q-q'+K)x}dx = E\sum_q a(q)\int_0^L e^{i(q-q')x}dx. \tag{4.16}$$

The Born–von Karman boundary conditions for a linear lattice lead to the conditions for the plane waves that $e^{iqx} = e^{iq(x+L)}$ and $e^{iq'x} = e^{iq'(x+L)}$. These conditions imply that both q and q' must satisfy

$$q = \frac{2\pi n}{L} \quad \text{and} \quad q' = \frac{2\pi m}{L}, \tag{4.17}$$

where n and m are integers. The integration

$$I = \int_0^L e^{i(q-q')x}dx = \frac{e^{i(q-q')L} - 1}{i(q-q')} = \frac{[e^{i2\pi(n-m)} - 1]L}{2\pi i(n-m)} = L\delta_{n,m} = L\delta_{q,q'}, \tag{4.18}$$

where $\delta_{q,q'}$ is the Kronecker delta function. Similarly, one can show that

$$I' = \int_0^L e^{i(q-q'+K)x}dx = L\delta_{q,q'-K}. \tag{4.19}$$

Substituting the results of Eqs. (4.18) and (4.19) in (4.16), we obtain

$$\varepsilon_q'^0 a(q') + \sum_K V(K)a(q'-K) = Ea(q'), \tag{4.20}$$

which can be written in the alternate form, by substituting q for q',

$$(\varepsilon_q^0 - E)a(q) + \sum_K V(K)a(q-K) = 0. \tag{4.21}$$

Eq. (4.21) can be expressed as

$$a(q) = \sum_K \frac{V(K)a(q-K)}{E - \varepsilon_q^0}. \tag{4.22}$$

It is obvious from Eq. (4.22) that $a(q)$ is small unless $E \approx \varepsilon_q^0$.

We can also subtract an arbitrary reciprocal lattice vector K' from q in Eq. (4.21) and rewrite it as

$$(\varepsilon^0_{q-K} - E)a(q-K') + \sum_K V(K)a(q-K'-K) = 0. \tag{4.23}$$

Eq. (4.22) connects $a(q)$ with every Fourier coefficient $a(q-K)$, i.e., with the Fourier coefficients for which the wave vector differs from q by a reciprocal lattice vector K. This leads to a very important and useful result about the form of the eigenfunctions ψ. These wave functions of an electron in a periodic potential are called the Bloch functions.

The equivalent proof correlating $a(\mathbf{q})$ and $a(\mathbf{q}-\mathbf{K})$ for a three-dimensional crystal lattice is assigned as a homework problem (see Problem 4.4).

4.2 BLOCH FUNCTIONS AND BLOCH THEOREM

In Eq. (4.12), we considered an arbitrary wave vector that appears in the summation over q and denoted it as k. We note from Eq. (4.21) that instead of the continuous Fourier coefficients $a(q)$, only those of the form $a(k-K)$ enter into $\psi_k(x)$; i.e., the allowed K's in the wave function are of the form $k-K$. Thus, we can write

$$\psi_k(x) = \sum_K a(k-K)e^{i(k-K)x}. \tag{4.24}$$

Eq. (4.24) can be written in the alternate form

$$\psi_k(x) = \left(\sum_K a(k-K)e^{-iKx}\right)e^{ikx}. \tag{4.25}$$

If we introduce

$$u_k(x) \equiv \sum_K a(k-K)e^{-iKx}, \tag{4.26}$$

we obtain

$$\psi_k(x) = e^{ikx}u_k(x). \tag{4.27}$$

We note from Eq. (4.26) that if m is an integer,

$$u_k(x+ma) = \sum_K a(k-K)e^{-iK(x+ma)} = u_k(x) \tag{4.28}$$

because

$$e^{-iKma} = e^{-2im\pi} = 1. \tag{4.29}$$

$\psi_k(x)$ is referred to as a Bloch function and $u_k(x)$ is known as the periodic part of the Bloch function because it has the periodicity of the lattice.

4.3 REDUCED, REPEATED, AND EXTENDED ZONE SCHEMES

We will now discuss the three types of zone schemes (reduced, repeated, and extended) used to describe electrons in a crystal lattice. For simplicity, we will first discuss these schemes for free electrons in a one-dimensional lattice to introduce the concept of the band index before we extend our discussion to electrons in a three-dimensional lattice as well as to electrons in a periodic potential.

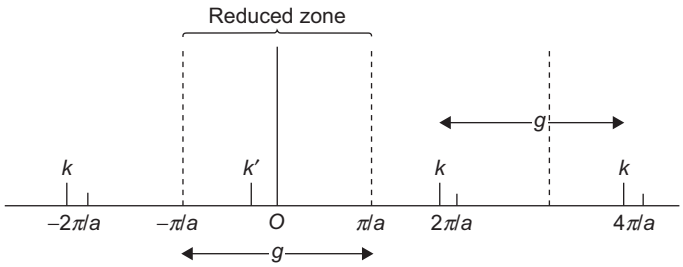

FIGURE 4.2

All k points reduce to k' in the one-dimensional reciprocal lattice.

4.3.1 Reduced Zone Scheme

If we consider a one-dimensional lattice, the reciprocal lattice vectors K can also be relabeled as g_n where n is an integer (positive or negative),

$$g_n = n\frac{2\pi}{a}. \tag{4.30}$$

If we restrict k to the first Brillouin zone, i.e., if we assign a state k, any wave number in the set

$$k = k' + \frac{2\pi}{a}n, \tag{4.31}$$

k is only defined modulo $(2\pi/a)$. Thus, all the k points in Figure 4.2 are equivalent.

One can therefore consider k' as the representative of all these k values, with $|k'|$ restricted to the first Brillouin zone. Thus, it is always possible to choose the value of k such that

$$-\frac{\pi}{a} < k \leq \frac{\pi}{a}. \tag{4.32}$$

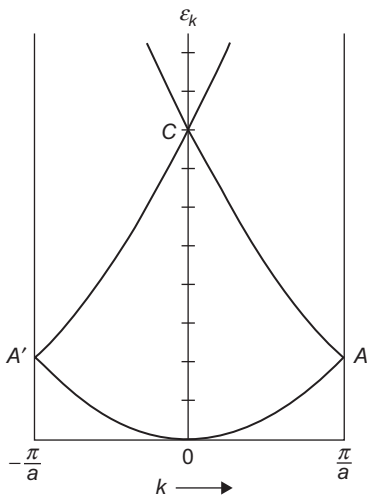

FIGURE 4.3

Reduced zone scheme for energy-wave number relations of free electrons in a one-dimensional lattice.

This way of restricting the wave numbers to the first Brillouin zone is known as the reduced zone scheme. In Figure 4.3, the reduced zone scheme is shown by drawing the energy-wave number relation for free electrons, $\varepsilon_0(k) = \hbar^2k^2/2m$.

We will now describe the energy-wave number relations $\varepsilon^0(k) = \hbar^2k^2/2m$ for the repeated and extended zone schemes.

4.3.2 Repeated Zone Scheme

It is often convenient to repeat the first Brillouin zone and the other zones reduced to the first Brillouin zone through all of k space. Thus, in the repeated zone scheme, $\varepsilon_k^0 = \varepsilon_{k+K}^0$ in one

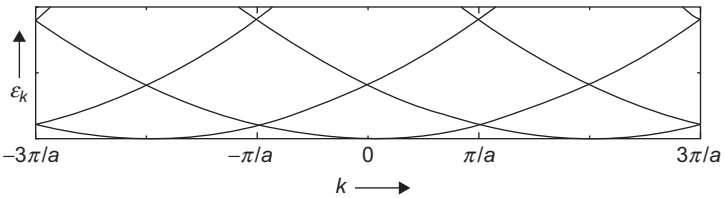

FIGURE 4.4

Energy-wave number relations for a one-dimensional lattice in the repeated zone scheme.

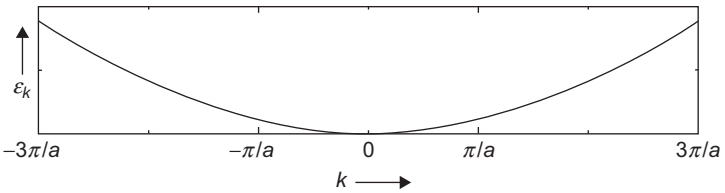

FIGURE 4.5

Energy-wave number relations in the extended zone scheme.

dimension and $\varepsilon^0_{\mathbf{k}} = \varepsilon^0_{\mathbf{k+K}}$ in three dimensions. All values of ε^0_k, ε^0_{k+K}, ε^0_{k-K}, etc. are plotted against k, $k+K$, $k-K$, etc. in one dimension. The repeated zone scheme is useful in describing several physical properties of the solid, specifically the connectivity of electron orbits in a magnetic field. The repeated zone scheme for free electrons in a one-dimensional lattice is shown schematically in Figure 4.4.

4.3.3 Extended Zone Scheme

In the extended zone scheme, the k values extend throughout all reciprocal space, and the energy eigenvalues, $\varepsilon^0_k = \hbar^2 k^2/2m$, are plotted against the wave number k. Thus, for free electrons, one obtains a parabola. The extended zone scheme for free electrons in a one-dimensional lattice is shown schematically in Figure 4.5.

4.4 BAND INDEX

A large number of eigenfunctions and eigenvalues correspond to the same wave vector $\mathbf{k}$ (wave numbers k in one dimension) in the reduced zone scheme. To distinguish these eigenfunctions and eigenvalues in the reduced zone scheme, we introduce an additional index n (called band index). The band index has a much greater significance when one considers the eigenfunctions and eigenvalues by including the periodic potential in the Hamiltonian. The periodic potential opens up an energy gap at the zone boundaries, and the band index plays a much greater role in the classification of solids as metals, insulators, and semiconductors. The necessity of using a band index also follows as a natural consequence when we discuss the effective Hamiltonian.

4.5 EFFECTIVE HAMILTONIAN

The necessity of a band index n will be evident by constructing an effective Hamiltonian. The Schrodinger equation can be written as

$$H\psi_{\mathbf{k}}(\mathbf{r}) = \left(-\frac{\hbar^2}{2m}\nabla^2 + V(\mathbf{r})\right)e^{i\mathbf{k}\cdot\mathbf{r}}u_{\mathbf{k}}(\mathbf{r}) = E_{\mathbf{k}}e^{i\mathbf{k}\cdot\mathbf{r}}u_{\mathbf{k}}(\mathbf{r}). \tag{4.33}$$

We can rewrite Eq. (4.33) in the form

$$e^{i\mathbf{k}\cdot\mathbf{r}}\left\{\frac{\hbar^2}{2m}[-\nabla^2 - 2i\mathbf{k}\cdot\overrightarrow{\nabla} + k^2]u_{\mathbf{k}}(\mathbf{r}) + V(\mathbf{r})u_{\mathbf{k}}(\mathbf{r})\right\} = e^{i\mathbf{k}\cdot\mathbf{r}}E_{\mathbf{k}}(\mathbf{r})u_{\mathbf{k}}(\mathbf{r}). \tag{4.34}$$

Canceling $e^{i\mathbf{k}\cdot\mathbf{r}}$ from both sides, we obtain

$$\left\{\frac{\hbar^2}{2m}[-\nabla^2 - 2i\mathbf{k}\cdot\overrightarrow{\nabla} + k^2] + V(\mathbf{r})\right\}u_{\mathbf{k}}(\mathbf{r}) = E_{\mathbf{k}}(\mathbf{r})u_{\mathbf{k}}(\mathbf{r}). \tag{4.35}$$

Eq. (4.35) can be expressed as

$$H_{eff}u_{\mathbf{k}}(\mathbf{r}) = E_{\mathbf{k}}(\mathbf{r})u_{\mathbf{k}}(\mathbf{r}), \tag{4.36}$$

where the effective Hamiltonian

$$H_{eff} = \frac{\hbar^2}{2m}[-\nabla^2 - 2i\mathbf{k}\cdot\nabla + k^2] + V(\mathbf{r}). \tag{4.37}$$

The boundary conditions are that whenever $\mathbf{r}$ lies on one boundary of the unit cell and $\mathbf{r}+\mathbf{R}$ is another boundary of the unit cell, then

$$u_{\mathbf{k}}(\mathbf{r}+\mathbf{R}) = u_{\mathbf{k}}(\mathbf{r}) \tag{4.38}$$

and

$$\hat{n}(\mathbf{r})\cdot\overrightarrow{\nabla}u_{\mathbf{k}}(\mathbf{r}) = -\hat{n}(\mathbf{r}+\mathbf{R})\cdot\overrightarrow{\nabla}u_{\mathbf{k}}(\mathbf{r}+\mathbf{R}), \tag{4.39}$$

where $\hat{n}(\mathbf{r})$ is a unit normal to the cell boundary at $\mathbf{r}$.

Thus, Eq. (4.36) can be considered as a Hermitian eigenvalue problem that is restricted to a single primitive cell of the crystal. Because the eigenvalue problem is in a fixed finite volume, there will be an infinite family of solutions with discretely spaced eigenvalues. These are labeled with the band index n. The importance of the band index will become apparent when we consider the effect of the periodic potential by using perturbation theory.

If we include the band index n, Eq. (4.27) can now be rewritten as

$$\psi_{nk}(x) = e^{ikx}u_{nk}(x). \tag{4.40}$$

It is easy to generalize Eq. (4.27) to a three-dimensional crystal lattice (see Problem 4.4),

$$\psi_{\mathbf{k}}(\mathbf{r}) = e^{i\mathbf{k}\cdot\mathbf{r}}u_{\mathbf{k}}(\mathbf{r}), \tag{4.41}$$

where

$$u_{\mathbf{k}}(\mathbf{r}+\mathbf{R}) = u_{\mathbf{k}}(\mathbf{r}). \tag{4.42}$$

For a three-dimensional lattice, in analogy with Eq. (4.31), we can write

$$\mathbf{k} = \mathbf{k}' + \mathbf{K}, \tag{4.43}$$

where $\mathbf{k}'$ is restricted to the first Brillouin zone. From Eq. (4.41) and (4.43), we obtain

$$\begin{aligned}\psi_{\mathbf{k}}(\mathbf{r}+\mathbf{R}_l) &= e^{i(\mathbf{k}'+\mathbf{K})\cdot\mathbf{R}_l}\psi_{\mathbf{k}}(\mathbf{r}) \\ &= e^{i\mathbf{K}\cdot\mathbf{R}_l}e^{i\mathbf{k}'\cdot\mathbf{R}_l}\psi_{\mathbf{k}}(\mathbf{r}) \\ &= e^{i\mathbf{k}'\cdot\mathbf{R}_l}\psi_{\mathbf{k}}(\mathbf{r}).\end{aligned} \tag{4.44}$$

From Eq. (4.44), it is evident that $\psi_{\mathbf{k}}(\mathbf{r})$ satisfies the Bloch's theorem with the wave vector $\mathbf{k}'$. Thus, every state has a large number of possible wave vectors, differing from each other by the reciprocal lattice vectors $\mathbf{K}$. If we choose the value of $\mathbf{K}$ such that $\mathbf{k}'$ lies in the first Brillouin zone (which is the reduced zone scheme, in which we relabel $\mathbf{k}'$ as $\mathbf{k}$), there will be a large number of eigenfunctions and eigenvalues corresponding to the same wave vector $\mathbf{k}$.

If we introduce the band index n, which follows as a consequence of restricting the wave vector $\mathbf{k}$ to the first Brillouin zone, Eq. (4.44) can be rewritten as

$$\psi_{n\mathbf{k}}(\mathbf{r}) = e^{i\mathbf{k}\cdot\mathbf{r}}u_{n\mathbf{k}}(\mathbf{r}) \tag{4.45}$$

and

$$u_{n\mathbf{k}}(\mathbf{r}+\mathbf{R}) = u_{n\mathbf{k}}(\mathbf{r}). \tag{4.46}$$

Eq. (4.45) is known as the Bloch theorem; $\psi_{n\mathbf{k}}(\mathbf{r})$ is known as the Bloch function, and $u_{n\mathbf{k}}(\mathbf{r})$ is known as the periodic part of the Bloch function. The Bloch theorem can also be proved by using the translational symmetry of the crystal lattice.

4.6 PROOF OF BLOCH'S THEOREM FROM TRANSLATIONAL SYMMETRY

We will now prove Bloch's theorem by using the translational symmetry of the crystal lattice. Through use of a three-dimensional equivalence of Problem 4.1, it can be easily shown that the translation operator $\hat{T}(\mathbf{R}_i)$ is defined by

$$\hat{T}(\mathbf{R}_i)f(\mathbf{r}) = f(\mathbf{r}+\mathbf{R}_i). \tag{4.47}$$

The Hamiltonian of the electron in the periodic potential can be written as

$$\hat{H}(\mathbf{r}) = \frac{-\hbar^2}{2m}\nabla^2 + V(\mathbf{r}). \tag{4.48}$$

From Eqs. (4.4), (4.47), and (4.48), we obtain

$$\hat{T}(\mathbf{R}_i)\hat{H}(\mathbf{r})f(\mathbf{r}) = \hat{H}(\mathbf{r}+\mathbf{R}_i)f(\mathbf{r}+\mathbf{R}_i) = \hat{H}(\mathbf{r})f(\mathbf{r}+\mathbf{R}_i) = \hat{H}(\mathbf{r})\hat{T}(\mathbf{R}_i)f(\mathbf{r}). \tag{4.49}$$

Because $f(\mathbf{r})$ is any arbitrary function of $\mathbf{r}$, we obtain

$$\hat{T}(\mathbf{R}_i)\hat{H}(\mathbf{r}) = \hat{H}(\mathbf{r})\hat{T}(\mathbf{R}_i). \tag{4.50}$$

It is also easy to show that

$$\hat{T}(\mathbf{R}_i)\hat{T}(\mathbf{R}_j)f(\mathbf{r}) = f(\mathbf{r}+\mathbf{R}_i+\mathbf{R}_j) = \hat{T}(\mathbf{R}_j)\hat{T}(\mathbf{R}_i)f(\mathbf{r}), \tag{4.51}$$

from which we have

$$\hat{T}(\mathbf{R}_i)\hat{T}(\mathbf{R}_j) = \hat{T}(\mathbf{R}_j)\hat{T}(\mathbf{R}_i) = \hat{T}(\mathbf{R}_i+\mathbf{R}_j). \tag{4.52}$$

From Eqs. (4.49) and (4.52), we note that the Hamiltonian $\hat{H}$ and the translation operators $\hat{T}(\mathbf{R}_i)$ (corresponding to each Bravais lattice vector $\mathbf{R}_i$) form a mutually commuting set of operators. Therefore, according to an important theorem in quantum mechanics,[5] these operators will have a complete set of common eigenfunctions.

If $\psi(\mathbf{r})$ is one of the eigenfunctions of the Hamiltonian with eigenvalue ε,

$$\hat{H}\psi(\mathbf{r}) = \varepsilon\psi(\mathbf{r}), \tag{4.53}$$

it follows from the previous theorem that

$$\hat{T}(\mathbf{R}_i)\psi(\mathbf{r}) = C(\mathbf{R}_i)\psi(\mathbf{r}) = \psi(\mathbf{r}+\mathbf{R}_i). \tag{4.54}$$

Here, $C(\mathbf{R}_i)$ are the eigenvalues of the translation operators $\hat{T}(\mathbf{R}_i)$. It also follows from Eq. (4.52) and Eq. (4.53) that

$$C(\mathbf{R}_i)C(\mathbf{R}_j) = C(\mathbf{R}_j)C(\mathbf{R}_i) = C(\mathbf{R}_i+\mathbf{R}_j). \tag{4.55}$$

Because $\mathbf{R}_i$ and $\mathbf{R}_j$ are Bravais lattice vectors, they can be expressed as

$$\mathbf{R}_i = n_1\mathbf{a}_1 + n_2\mathbf{a}_2 + n_3\mathbf{a}_3$$

and

$$\mathbf{R}_j = m_1\mathbf{a}_1 + m_2\mathbf{a}_2 + m_3\mathbf{a}_3, \tag{4.56}$$

where $\mathbf{a}_1, \mathbf{a}_2$, and $\mathbf{a}_3$ are the three primitive vectors of the Bravais lattice and n_1, n_2, n_3, m_1, m_2, and m_3 are appropriate integers corresponding to the lattice vectors $\mathbf{R}_i$ and $\mathbf{R}_j$. From Eqs. (4.55) and (4.56), it is obvious that $C(\mathbf{a}_i)$ must be an exponential of the form

$$C(\mathbf{a}_i) = e^{p_i}, \tag{4.57}$$

where p_i, which could be a complex number, has to be determined. From Eqs. (4.56) and (4.57), we obtain

$$C(\mathbf{R}_i) = C(\mathbf{a}_1)^{n_1}C(\mathbf{a}_2)^{n_2}C(\mathbf{a}_3)^{n_3}. \tag{4.58}$$

From Eqs. (4.57) and (4.58), we obtain

$$C(\mathbf{R}_i) = e^{n_1p_1+n_2p_2+n_3p_3}. \tag{4.59}$$

We now restate the Born–von Karman boundary conditions (originally stated for a cubic crystal in Eq. 3.11) for the wave functions of the electrons in a more general form (instead of restricting these conditions to a cubic crystal),

$$\psi(\mathbf{r}+M_i\mathbf{a}_i) = e^{M_ip_i}\psi(\mathbf{r}) = \psi(\mathbf{r}), \quad i = 1, 2, 3, \tag{4.60}$$

where M_1, M_2, and M_3 are the number of primitive vectors in the directions $\mathbf{a}_1$, $\mathbf{a}_2$, and $\mathbf{a}_3$, respectively. Obviously, the total number of primitive cells in the crystal

$$N = M_1M_2M_3. \tag{4.61}$$

From Eq. (4.61), we obtain

$$e^{M_1p_1} = e^{M_2p_2} = e^{M_3p_3} = 1. \tag{4.62}$$

Eq. (4.62) yields the necessary condition that

$$p_i = \frac{2\pi i m_i}{M_i} \cdot i = 1,\ 2,\ 3, \tag{4.63}$$

where, m_1, m_2, and m_3 are a set of integers. If we define the Bloch wave vectors as

$$\mathbf{k} = \sum_{i=1}^{3} \frac{p_i}{2\pi i}\mathbf{b}_i, \quad 0 \le m_i < M_i, \tag{4.64}$$

where $\mathbf{b}_i$, the primitive vectors of the reciprocal lattice, were defined in Eq. (1.16).

According to Eq. (4.64), the total number of $\mathbf{k}$ states in a Brillouin zone is $M_1M_2M_3$, which is also equal to the number of lattice points in the lattice. It is possible to have $\mathbf{k}$ outside the first Brillouin zone by allowing the integers to be greater than M_i. However, the resulting $\mathbf{k}$ would differ from the $\mathbf{k}$ within the first Brillouin zone by a reciprocal lattice vector $\mathbf{K}$. Because $e^{i\mathbf{k}\cdot\mathbf{R}_i} = e^{i(\mathbf{k}+\mathbf{K})\cdot\mathbf{R}_i}$, the resulting eigenfunction would be the same according to Eq. (4.45) as well as from Eq. (4.67) (which we will prove), and because $\mathbf{k}$ is a label for this eigenvalue, two such $\mathbf{k}$ values are physically identical. Thus, the number of physically distinct values of the Bloch wave vector $\mathbf{k}$ equals the number of lattice sites of the original Bravais lattice.

We obtain from Eqs. (4.60), (4.63), and (4.64),

$$e^{iM_i\mathbf{k}\cdot\mathbf{a}_i} = 1 \tag{4.65}$$

and

$$C(\mathbf{R}_i) = e^{i\mathbf{k}\cdot\mathbf{R}_i}. \tag{4.66}$$

We obtain from Eqs. (4.52) and (4.66), the Bloch theorem,

$$\psi(\mathbf{r}+\mathbf{R}_i) = C(\mathbf{R}_i)\psi(\mathbf{r}) = e^{i\mathbf{k}\cdot\mathbf{R}_i}\psi(\mathbf{r}). \tag{4.67}$$

If we identify the eigenfunctions $\psi(\mathbf{r})$ with a band index n and wave vector $\mathbf{k}$ (we will show the importance and the necessity of the band index), Eq. (4.67) can be written in the more general form

$$\psi_{n\mathbf{k}}(\mathbf{r}+\mathbf{R}_i) = e^{i\mathbf{k}\cdot\mathbf{R}_i}\psi_{n\mathbf{k}}(\mathbf{r}). \tag{4.68}$$

The Bloch theorem stated in Eq. (4.68) can also be rewritten in the alternate form

$$\psi_{n\mathbf{k}}(\mathbf{r}) = e^{i\mathbf{k}\cdot\mathbf{r}}u_{n\mathbf{k}}(\mathbf{r}), \tag{4.69}$$

where $u_{n\mathbf{k}}(\mathbf{r})$ is known as the periodic part of the Bloch function. In fact, from Eqs. (4.68) and (4.69), we obtain

$$u_{n\mathbf{k}}(\mathbf{r}+\mathbf{R}_i) = u_{n\mathbf{k}}(\mathbf{r}), \tag{4.70}$$

from which the term *periodic part* is self-evident.

4.7 APPROXIMATE SOLUTION NEAR A ZONE BOUNDARY

To understand the occurrence of band gaps, we consider the results of Problem 4.4 (Eq. 10),

$$(\varepsilon^0_{\mathbf{k}-\mathbf{K}} - \varepsilon)C_{\mathbf{k}-\mathbf{K}} + \sum_{\mathbf{K}'} V_{\mathbf{K}'-\mathbf{K}}C_{\mathbf{k}-\mathbf{K}'} = 0, \tag{4.71}$$

where

$$\varepsilon^0_{\mathbf{k}-\mathbf{K}} \equiv \frac{\hbar^2(\mathbf{k}-\mathbf{K})^2}{2m} \tag{4.72}$$

is the free electron energy eigenvalue for an electron of wave vector $\mathbf{k} - \mathbf{K}$. We will also denote $\varepsilon^0_{\mathbf{k}}$ as the free electron eigenvalue for wave vector $\mathbf{k}$.

We can rewrite Eq. (4.71) as

$$(\varepsilon - \varepsilon^0_{\mathbf{k}-\mathbf{K}})C_{\mathbf{k}-\mathbf{K}} = \sum_{\mathbf{K}' \neq \mathbf{K}} V_{\mathbf{K}'-\mathbf{K}} C_{\mathbf{k}-\mathbf{K}'} \tag{4.73}$$

because we have assumed that $V_0 = 0$. Eq. (4.73) includes the terms $\mathbf{K} = 0$ and $\mathbf{K}' = 0$. If we use nondegenerate perturbation theory and assume that

$$\left|\varepsilon^0_{\mathbf{k}-\mathbf{K}} - \varepsilon^0_{\mathbf{k}-\mathbf{K}'}\right| \gg V_{\mathbf{K}'-\mathbf{K}}, \tag{4.74}$$

for all $\mathbf{K}' \neq \mathbf{K}$ and fixed $\mathbf{k}$, Eq. (4.73) can be rewritten as

$$C_{\mathbf{k}-\mathbf{K}} = \sum_{\mathbf{K}' \neq \mathbf{K}} \frac{V_{\mathbf{K}'-\mathbf{K}} C_{\mathbf{k}-\mathbf{K}'}}{\varepsilon - \varepsilon^0_{\mathbf{k}-\mathbf{K}}}. \tag{4.75}$$

For another coefficient $C_{\mathbf{k}-\mathbf{K}_1}$ corresponding to the reciprocal lattice vector $\mathbf{K}_1$ (where $\mathbf{K}_1$ satisfies the condition of Eq. 4.74),

$$C_{\mathbf{k}-\mathbf{K}_1} = \frac{V_{\mathbf{K}-\mathbf{K}_1} C_{\mathbf{k}-\mathbf{K}}}{\varepsilon - \varepsilon^0_{\mathbf{k}-\mathbf{K}_1}} + \sum_{\mathbf{K}' \neq \mathbf{K} \neq \mathbf{K}_1} \frac{V_{\mathbf{K}'-\mathbf{K}_1} C_{\mathbf{k}-\mathbf{K}'}}{\varepsilon - \varepsilon^0_{\mathbf{k}-\mathbf{K}'}}. \tag{4.76}$$

In deriving Eq. (4.76), we have made the basic assumption that the free electron eigenvalue $\varepsilon^0_{\mathbf{k}-\mathbf{K}}$ is not nearly degenerate to any other $\varepsilon^0_{\mathbf{k}-\mathbf{K}'}$ in the set. Otherwise, the expansion of the energy in Eq. (4.78) in second order and higher terms in V would not be valid.

From Eqs. (4.73) and (4.76), we obtain

$$\begin{aligned}(\varepsilon - \varepsilon^0_{\mathbf{k}-\mathbf{K}})C_{\mathbf{k}-\mathbf{K}} = {} & \sum_{\mathbf{K}' \neq \mathbf{K}} \frac{V_{\mathbf{K}'-\mathbf{K}} V_{\mathbf{K}-\mathbf{K}'}}{\varepsilon - \varepsilon^0_{\mathbf{k}-\mathbf{K}'}} C_{\mathbf{k}-\mathbf{K}} + \sum_{\mathbf{K}'' \neq \mathbf{K}' \neq \mathbf{K}} \frac{V_{\mathbf{K}'-\mathbf{K}} V_{\mathbf{K}-\mathbf{K}'} V_{\mathbf{K}-\mathbf{K}''}}{(\varepsilon - \varepsilon^0_{\mathbf{k}-\mathbf{K}'})(\varepsilon - \varepsilon^0_{\mathbf{k}-\mathbf{K}''})} C_{\mathbf{k}-\mathbf{K}} \\ & + \text{higher-order terms in } V.\end{aligned} \tag{4.77}$$

Because the perturbed energy ε differs from the free electron energy $\varepsilon^0_{\mathbf{k}-\mathbf{K}}$ by $|V|^2$ or higher-order terms (in the specific case of energy values that are neither degenerate nor nearly degenerate), we retain the terms up to the second order in V, use the relation $V_{-\mathbf{K}} = V^*_{\mathbf{K}}$ in Eq. (4.77), substitute ε by $\varepsilon^0_{\mathbf{k}-\mathbf{K}}$ in the denominator of the first term on the right, and obtain the expression for ε:

$$\varepsilon = \varepsilon^0_{\mathbf{k}-\mathbf{K}} + \sum_{\mathbf{K}' \neq \mathbf{K}} \frac{|V_{\mathbf{K}'-\mathbf{K}}|^2}{\varepsilon^0_{\mathbf{k}-\mathbf{K}} - \varepsilon^0_{\mathbf{k}-\mathbf{K}'}} + O(V^3). \tag{4.78}$$

Eq. (4.78) is valid as long as nondegenerate perturbation theory can be applied to the problem, i.e., as long as $\varepsilon^0_{\mathbf{k}-\mathbf{K}} \neq \varepsilon^0_{\mathbf{k}-\mathbf{K}'}$ (or sufficiently close in values so that the perturbation theory breaks down). The simplest example is when $\mathbf{k}$ lies near a zone boundary, in which case the second-order perturbation theory breaks down.

If $\mathbf{k}$ lies near a zone boundary (for simplicity, we assume that it lies near the boundary bisecting the vector $\mathbf{K}$), the electron undergoes a Bragg reflection by the lattice, similar to the situation as if it would have been an external electron beam. In such a case, we will use degenerate perturbation theory, consider only $C_{\mathbf{k}}$ and $C_{\mathbf{k}-\mathbf{K}}$, and neglect the other coefficients.

Eq. (4.73) can be rewritten as

$$\begin{aligned}(\varepsilon_{\mathbf{k}}^0 - \varepsilon)C_{\mathbf{k}} + V_{\mathbf{K}}C_{\mathbf{k}-\mathbf{K}} &= 0\\ V_{-\mathbf{K}}C_{\mathbf{k}} + (\varepsilon_{\mathbf{k}-\mathbf{K}}^0 - \varepsilon)C_{\mathbf{k}-\mathbf{K}} &= 0.\end{aligned} \tag{4.79}$$

From Eqs. (4.77) and (4.79), we obtain

$$\begin{aligned}(\varepsilon_{\mathbf{k}}^0 - \varepsilon)C_{\mathbf{k}} + V_{\mathbf{K}}C_{\mathbf{k}-\mathbf{K}} &= 0\\ V_{\mathbf{K}}^*C_{\mathbf{k}} + (\varepsilon_{\mathbf{k}-\mathbf{K}}^0 - \varepsilon)C_{\mathbf{k}-\mathbf{K}} &= 0.\end{aligned} \tag{4.80}$$

We have $\varepsilon_{\mathbf{k}}^0 \approx \varepsilon_{\mathbf{k}-\mathbf{K}}^0$ and $|\varepsilon_{\mathbf{k}}^0 - \varepsilon_{\mathbf{k}-\mathbf{K}}^0| \gg V$, when $\mathbf{K} \neq \mathbf{K}, \mathbf{0}$. This is possible only when $|\mathbf{k}-\mathbf{K}| = |\mathbf{k}|$. It is evident from Figure 4.6(a) that this is possible only when $\mathbf{k}$ lies on the Bragg plane that bisects the line joining the origin of $\mathbf{k}$ space to the reciprocal lattice point $\mathbf{K}$.

Eq. (4.80) can be solved from the determinant

$$\begin{vmatrix} \varepsilon_{\mathbf{k}}^0 - \varepsilon & V_{\mathbf{K}} \\ V_{\mathbf{K}}^* & \varepsilon_{\mathbf{k}-\mathbf{K}}^0 - \varepsilon \end{vmatrix} = 0. \tag{4.81}$$

The solutions of the quadratic equation are

$$\varepsilon^{\pm}(\mathbf{k}) = \frac{1}{2}(\varepsilon_{\mathbf{k}}^0 + \varepsilon_{\mathbf{k}-\mathbf{K}}^0) \pm \left[\left(\frac{\varepsilon_{\mathbf{k}}^0 - \varepsilon_{\mathbf{k}-\mathbf{K}}^0}{2}\right)^2 + |V_{\mathbf{K}}|^2\right]^{\frac{1}{2}}. \tag{4.82}$$

Thus, the free electron states $e^{i\mathbf{k}\cdot\mathbf{r}}$ and $e^{i(\mathbf{k}-\mathbf{K})\cdot\mathbf{r}}$ with energy $\varepsilon_{\mathbf{k}}^0$ and $\varepsilon_{\mathbf{k}-\mathbf{K}}^0$ are combined into two other states ψ^+ and $\psi-$ with energy $\varepsilon+(\mathbf{k})$ and $\varepsilon-(\mathbf{k})$.

It is easy to analyze Eq. (4.82) for points lying on the Bragg plane because $|\mathbf{k}| = |\mathbf{k}-\mathbf{K}|$ and $\varepsilon_{\mathbf{k}}^0 = \varepsilon_{\mathbf{k}-\mathbf{K}}^0$. This implies that $\mathbf{k}$ must lie on the Brillouin zone boundary (see Figure 4.6a). Further, at all points on the Bragg plane, one energy level is raised by $|V_{\mathbf{K}}|$, whereas the other energy level is lowered by $|V_{\mathbf{K}}|$. Thus, when $\mathbf{k}$ is on a single Bragg plane, we can write

$$\varepsilon^{\pm}(\mathbf{k}) = \varepsilon_{\mathbf{k}}^0 \pm |V_{\mathbf{K}}|. \tag{4.83}$$

Hence, there is an energy gap of $2|V_{\mathbf{k}}|$ when $\mathbf{k} = \frac{1}{2}\mathbf{K}$. This is shown in Figure 4.7. This is known as the band gap because the energy levels are split into two bands. When $\mathbf{k}$ is closer to the origin (far away from the Bragg plane), the energy levels are practically the same as the free electron energy levels.

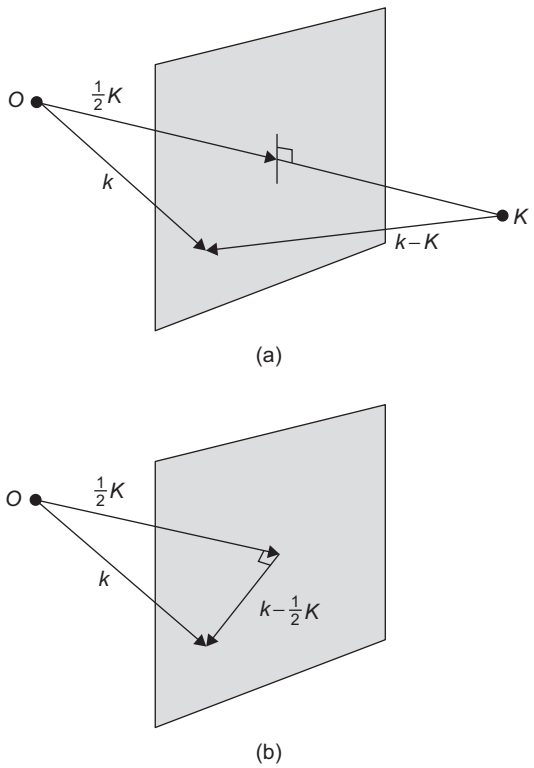

FIGURE 4.6

(a) $\mathbf{k}$ lies in the Bragg plane determined by $\mathbf{K}$ if $|\mathbf{k}| = |\mathbf{k}-\mathbf{K}|$; (b) $\mathbf{k} - \frac{1}{2}\mathbf{K}$ is parallel to the Bragg plane if $\mathbf{k}$ lies in the Bragg plane.

In addition, when $\varepsilon^0_{\mathbf{k}} = \varepsilon^0_{\mathbf{k}-\mathbf{K}}$, we obtain from Eq. (4.82),

$$\frac{\partial \varepsilon}{\partial \mathbf{k}} = \frac{\hbar^2}{m}\left(\mathbf{k} - \frac{1}{2}\mathbf{K}\right). \tag{4.84}$$

Eq. (4.84) implies that when $\mathbf{k}$ is on the Bragg plane, the gradient of ε is parallel to the Bragg plane (see Figure 4.6b). Therefore, the constant-energy surfaces at the Bragg plane are perpendicular to the plane because the gradient is perpendicular to the surfaces on which a function is constant.

It is easy to plot the energy bands from Eq. (4.82) if $\mathbf{k}$ is parallel to $\mathbf{K}$ (see Figure 4.7). When $\mathbf{k} = \frac{1}{2}\mathbf{K}$, the two bands are separated by a band gap $2|V_{\mathbf{k}}|$.

It is much easier to consider the energy bands in one dimension. In one dimension, if we consider $\mathbf{k}$ at the zone boundary at $\frac{1}{2}\mathbf{K}$, we note that $(\mathbf{k}-\mathbf{K})^2 = \mathbf{k}^2$ and $\varepsilon^0_k = \varepsilon^0_{k-K}$. Thus, in Eqs. (4.20) and (4.23), we retain only the terms involving $a(k)$ and $a(k-K)$ and write $E = \varepsilon(k)$, and we obtain

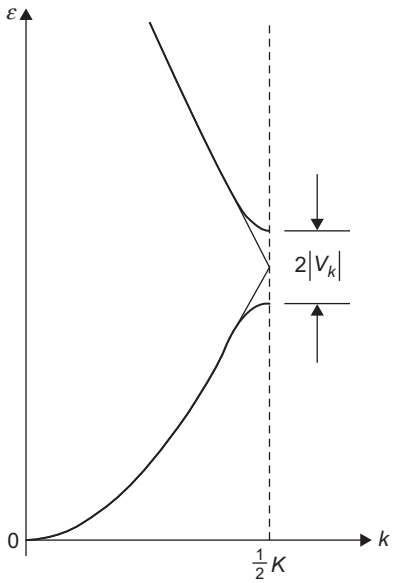

FIGURE 4.7
Energy bands when $\mathbf{k}$ is parallel to $\mathbf{K}$.

$$(\varepsilon^0_k - \varepsilon(k))a(k) + V_K a(k-K) = 0, \tag{4.85}$$

$$V_{-K}a(k) + (\varepsilon^0_{k-K} - \varepsilon(k))a(k-K) = 0. \tag{4.86}$$

Because $V_K = V_{-K} = V_K*$, Eqs. (4.85) and (4.86) can be solved by the determinant equation

$$\begin{vmatrix} \varepsilon^0_k - \varepsilon(k) & V_K \\ V^*_K & \varepsilon^0_{k-K} - \varepsilon(k) \end{vmatrix} = 0, \tag{4.87}$$

which can be rewritten as

$$\varepsilon(k)^2 - \varepsilon(k)(\varepsilon^0_{k-K} + \varepsilon^0_k) + \varepsilon^0_{k-K}\varepsilon^0_k - |V_K|^2 = 0. \tag{4.88}$$

Thus, the two roots are

$$\varepsilon^{\pm}(k) = \frac{1}{2}(\varepsilon^0_{k-K} + \varepsilon^0_k) \pm \left[\tfrac{1}{4}(\varepsilon^0_{k-K} - \varepsilon^0_k)^2 + |V_K|^2\right]^{\frac{1}{2}}. \tag{4.89}$$

When $\mathbf{k} = \mathbf{K}/2$ (at the zone boundary),

$$\varepsilon^{\pm}(K/2) = \varepsilon^0_{K/2} \pm |V_K|. \tag{4.90}$$

Substituting Eq. (4.90) in Eqs. (4.85) and (4.86), we obtain

$$|\pm V_K|a(K/2) = -V_K a(-K/2), \tag{4.91}$$

for the two roots marked $\pm$.

The corresponding eigenstates $\psi^{\pm}(r)$ are obtained from Eqs. (4.24), (4.85), and (4.86). When $\mathbf{k} = \mathbf{K}/2$, assuming that V_K is negative, $a(K/2) = a(-K/2)$ for the negative root and $a(K/2) = -a(-K/2)$ for the positive root. Thus, we obtain

$$\psi^{-}(r) = a(K/2)[e^{i/2Kr} + e^{-i/2Kr}] \tag{4.92}$$

and

$$\psi^{+}(r) = a(K/2)[e^{i/2Kr} - e^{-i/2Kr}]. \tag{4.93}$$

Using the normalization conditions for the eigenstates, we obtain

$$\psi^{-}(r) = \frac{1}{\sqrt{2}}[e^{i/2Kr} + e^{-i/2Kr}] = \sqrt{2}\cos\frac{1}{2}Kr, \tag{4.94}$$

and

$$\psi^{+}(r) = \frac{1}{\sqrt{2}}[e^{i/2Kr} - e^{-i/2Kr}] = \sqrt{2}i\sin\frac{1}{2}Kr. \tag{4.95}$$

When k is near the zone boundary, we can define a wave vector δ, which measures the difference of k from the zone boundary by

$$\delta = K/2 - k. \tag{4.96}$$

From Eqs. (4.89) and (4.96), we obtain

$$\begin{aligned}\varepsilon^{\pm}(k) &= (\hbar^2/2m)\left(\frac{1}{4}K^2 + \delta^2\right) \pm [4\varepsilon^0_{K/2}(\hbar^2\delta^2/2m) + |V_K|^2]^{\frac{1}{2}} \\ &\cong (\hbar^2/2m)\left(\frac{1}{4}K^2 + \delta^2\right) \pm |V_K|[1 + 2(\varepsilon^0_{K/2}/|V_K|^2)(\hbar^2\delta^2/2m)]^{\frac{1}{2}}.\end{aligned} \tag{4.97}$$

From Eqs. (4.90) and (4.97), we obtain

$$\varepsilon^{\pm}(k) = \varepsilon^{\pm}(K/2) + (\hbar^2\delta^2/2m)[1 \pm 2(\varepsilon^0_{K/2}/|V_K|^2]. \tag{4.98}$$

When $k \sim 0$, or far from a zone boundary (in the extended zone scheme),

$$\varepsilon(k) \sim \varepsilon^0_k \sim \hbar^2k^2/2m, \tag{4.99}$$

which is a free electron parabola. We will represent these results in the reduced, extended, and repeated zone schemes described earlier for free electrons.

4.8 DIFFERENT ZONE SCHEMES

4.8.1 Reduced Zone Scheme

In the reduced zone scheme, the wave vector $\mathbf{k}$ always lies within the first Brillouin zone. If a wave vector $\mathbf{k}'$ lies outside the first Brillouin zone, one can always find a lattice vector $\mathbf{K}'$ such that $\mathbf{k} = \mathbf{k}' - \mathbf{K}'$ lies within the first Brillouin zone. We show in Figure 4.8 the energy bands of a linear lattice (with a periodic potential) in the reduced zone scheme.

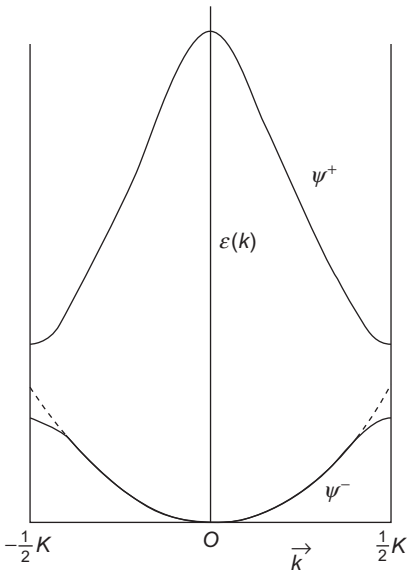

FIGURE 4.8

The energy bands of a linear lattice in the reduced zone scheme.

4.8.2 Extended Zone Scheme

In the extended zone scheme, the energy $\varepsilon(\mathbf{k})$ is plotted against the wave vector $\mathbf{k}$. We had seen that for free electrons, the curve is the free electron parabola because $\varepsilon(\mathbf{k}) = \frac{\hbar^2 k^2}{2m}$.

However, in the presence of a periodic potential, as we have seen, the parabola must meet the zone boundary normally, and an energy gap of $2|V_K|$ develops between the lower and the upper band. This gap increases as $\mathbf{K}$ increases. The energy bands in the extended zone scheme of a linear lattice with periodic potential are shown in Figure 4.9.

Figure 4.10 shows the energy bands for a linear lattice with periodic potential and succinctly demonstrates the development of the forbidden part of the zone (or more commonly referred to as band gap) that increases as the energy of the band increases.

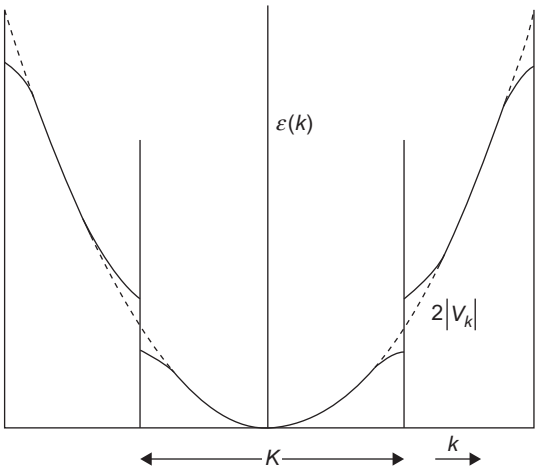

FIGURE 4.9

The energy bands of a linear lattice in the extended zone scheme.

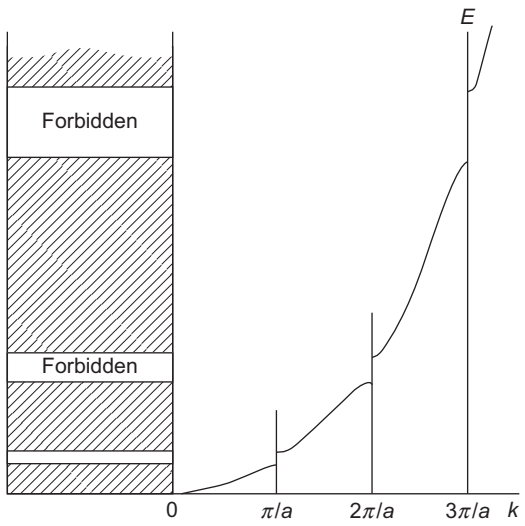

FIGURE 4.10

The energy gaps in a linear lattice. The width in energy increases as the energy of the band increases. In pure materials, there are no eigenstates for electrons with energy lying within these energy gaps.

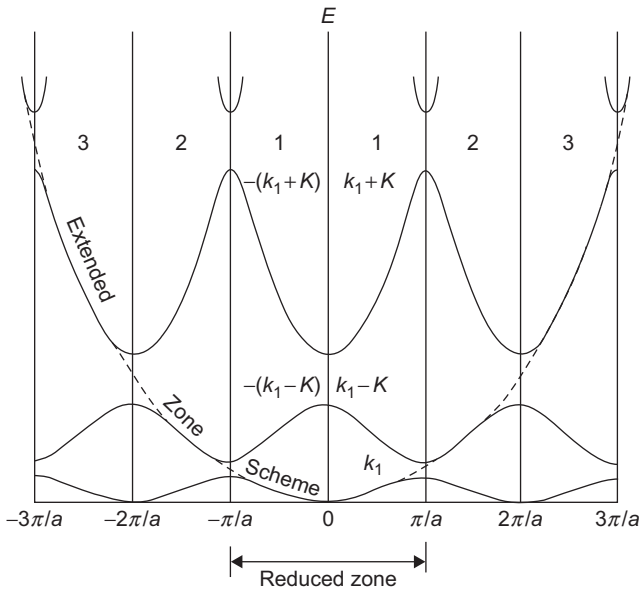

FIGURE 4.11

The repeated zone scheme for a linear lattice and its comparison with the reduced and extended zone schemes shown in Figures 4.9 and 4.10.

4.8.3 Repeated Zone Scheme

When the first Brillouin zone is periodically repeated through all $\mathbf{k}$ space, $\varepsilon(\mathbf{k}) = \varepsilon(\mathbf{k}+\mathbf{K})$. In fact, $\varepsilon(\mathbf{k}+\mathbf{K})$ is the same energy band as $\varepsilon(\mathbf{k})$. This type of construction of energy bands is known as the repeated zone scheme. This scheme is particularly useful in demonstrating the electron orbits in a magnetic field. The repeated zone scheme and its connection with the reduced and extended zone schemes is shown in Figure 4.11.

4.9 ELEMENTARY BAND THEORY OF SOLIDS

4.9.1 Introduction

We will now discuss the elementary band theory of solids using the one-dimensional lattice and analyze how crystalline solids, of which the basic components are negatively charged electrons and positively charged ions, have a wide diversity in physical properties. For example, some solids are metals that are good conductors, some others are metals but poor conductors, some crystallize as insulators, and the rest are crystals that are semiconductors. Each of these types of solids has widely divergent properties. For example, whereas some metals such as the alkali metals are very good conductors, some others such as the alkaline-earth metals are comparatively poor conductors. Another striking feature is that the ratio of the resistivity of metals (good conductors) and insulators is of the order of 10^{-20} at room temperature. As has been often remarked, this is one of the widest

divergences in the physical properties occurring in nature. Another example is the difference between the temperature dependence of the resistivity of metals and semiconductors. The resistivity of metals, which is small at absolute zero, increases with increase of temperature. In contrast, the resistivity of pure semiconductors, which are insulators (if the material is pure) at absolute zero, decreases with increase of temperature. We will try to explain this wide variety of exotic properties by using a simple one-dimensional band theory. In subsequent chapters, we will discuss the various techniques used in the energy band theory of solids in three dimensions and discuss the properties of various types of solids in a more rigorous manner.

4.9.2 Energy Bands in One Dimension

We have discussed how a periodic potential breaks the free electron energy curve, which is a parabola, into discrete segments of interval π/a. Thus, there is a forbidden region for eigenstates of electrons in pure materials that is known as the energy gap. This energy gap increases with the increase in energy; i.e., the higher the energy of the band, the larger its width in energy. This significant fact, which is essentially the elementary band theory of solids, allows us to understand many of the characteristic features of solids. The basic idea of the formation of these energy bands was shown in Figure 4.10.

4.9.3 Number of States in a Band

Here, we consider a one-dimensional crystal constructed of primitive cells of lattice constant a. The length of the crystal is $L = Na$, where N is the number of primitive cells. As we have noted, in one dimension, the allowed values of the electron wave vector $\mathbf{k}$ in the first Brillouin zone are given by

$$k = 0; \pm\frac{2\pi}{L}; \pm\frac{4\pi}{L}; \ldots, \frac{N\pi}{L}. \tag{4.100}$$

We note that because $N\pi/L \equiv \pi/a$, the point, defined as $-N\pi/L \equiv -\pi/a$, is connected by a reciprocal lattice vector K with π/a, and hence cannot be counted as an independent point. The total number of points given in Eq. (4.100) is N. This result is also carried over to three dimensions; i.e., each primitive cell contributes one independent value of k to each energy band. If one considers the spin of the electron, each energy band will have $2N$ independent states.

4.10 METALS, INSULATORS, AND SEMICONDUCTORS

We can now discuss the reason crystalline solids have to be grouped into four extremely dissimilar varieties: metals (good conductors), semimetals (poor conductors), insulators, and semiconductors. First, by using the elementary band theory, we will discuss some of the general features that are responsible for distinguishing solids into these four categories. Later, we will discuss some specific examples in each category to illustrate the characteristic features.

If there is a single atom of valence one in each primitive cell, the first band (the bands are stacked above each other with [increasing] energy gaps between them, as shown in Figure 4.11) will be half-filled with electrons, and the solid will be a metal (good conductor) because there are enough empty states available for electrons to be excited whenever an electric field $\mathbf{E}$ is applied. In

fact, when an electric field **E** is applied, the force on the electron of charge $-e$ is $\mathbf{F} = -e\mathbf{E}$. The force is also the rate of change of momentum,

$$\mathbf{F} = -e\mathbf{E} = \hbar \frac{d\mathbf{k}}{dt}. \tag{4.101}$$

Because the alkali metals and noble metals have one valence electron per primitive cell, they are good conductors. As an example, we consider sodium. Each Na atom has the atomic configuration $1s^2 2s^2 2p^6 3s^1$. Thus, there is one valence electron in the $3s$ state in each separated Na atom, while the $3s$ state could accommodate two valence electrons. When N such atoms are bound in a solid, the $3s$ energy band has N electrons, and therefore, it is only half-filled (a band can accommodate $2N$ electrons). Thus, sodium is a good conductor because there are a large number of energy levels available just above the filled ones and the valence electrons can be easily raised to a higher energy state by an electric field, as shown in Eq. (4.101). In fact, as a rule of thumb, all monovalent solids are good conductors.

According to the same rule of thumb, all divalent solids like the alkaline-earth metals that have two valence electrons per primitive cell should be insulators. However, this is not true if we consider a three-dimensional band picture. For example, we consider magnesium, of which the atomic configuration is $1s^2 2s^2 2p^6 3s^2$. The $3s$ energy band is full, and as per the one-dimensional band picture, magnesium should be an insulator. However, this is not true because in a three-dimensional band picture, there is an overlap between the $3s$ and $3p$ bands, which is shown in Figure 4.12. In fact, the same overlap was also there for sodium in a three-dimensional band picture, but we did not have to take that fact into consideration because the $3s$ band was only half full. Because of this overlap between $3s$ and $3p$ bands, magnesium, like all alkaline-earth metals, is a metal, but some

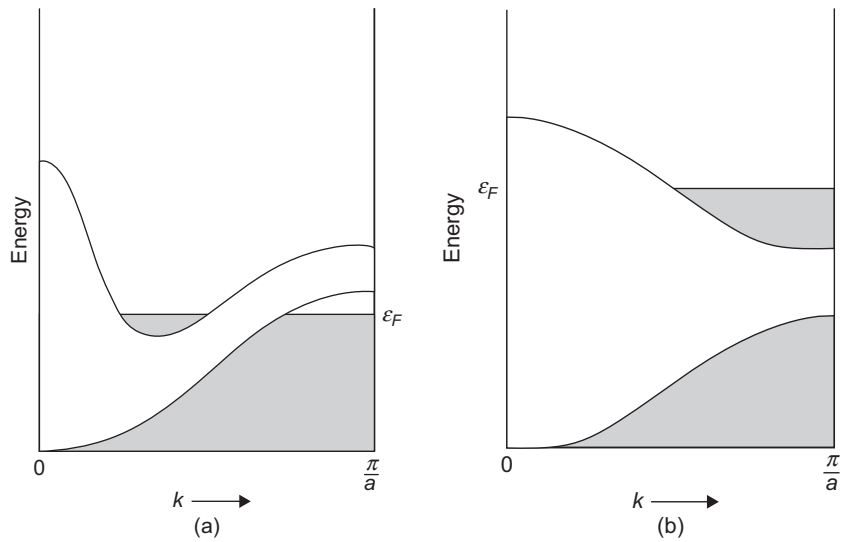

FIGURE 4.12

(a) The overlap of the $3s$ and $3p$ energy bands in three dimensions. (b) In Al, the $3s$ band is full, but the $3p$ band is not full. The upper energy level is the Fermi energy ε_F.

divalent solids such as Sr and Ba are poor conductors because the overlap is small and a relatively small number of electrons are excited when an electric field is applied.

We note in Figure 4.12a that the three components of the wave vector **k** are in different directions in the 3*s* and 3*p* bands. Thus, the lowest energy levels of the 3*p* band are lower in energy than the highest energy levels of the 3*s* band, a fact that would be impossible in a one-dimensional band picture. Because the electrons tend to occupy the lowest energy states, some electrons have spilled over to the 3*p* band. We also note that the highest energy level in both bands is the Fermi level ε_F, which is in conformity with the definition of the Fermi level.

All trivalent solids such as Al, Ga, In, and Tl are good metals because there are three valence electrons per primitive cell, and hence, they can fill one and a half bands. For example, the atomic configuration of aluminum is $1s^2 2s^2 2p^6 3s^2 3p^1$. The valence electrons are in the 3*p* band that is half empty and can be easily excited to higher energy states by an electric field. Therefore, aluminum is a very good conductor. This is schematically shown in Figure 4.12b.

A crystalline solid becomes an insulator if it has only completely filled bands, provided the energy gap between the last-filled band (known as the valence band) and the next allowed empty band (known as the conduction band) is very large. The condition that the energy gap between the valence and conduction bands must be very large is due to the fact that the electrons can be thermally excited to the conduction band at room temperature if the energy gap is small. In addition, when an electric field is applied, the electrons are excited due to the external force (Eq. 4.101). The energy gap has to be large enough to prevent the excitation of the electrons from the valence band to the conduction band at reasonably large electric fields. The ionic crystals are good examples of insulators. The energy bands of an ionic crystal such as NaCl are from the Na^+ $(1s^2 2s^2 2p^6)$ and Cl^- $(1s^2 2s^2 2p^6 3s^2 3p^6)$ ions. Because both of these ions have a closed-shell structure, all the occupied bands of NaCl are full and the energy gap between the highest occupied band (valence band) and the next empty (conduction) band is very large. Another example of an insulator that is a tetravalent solid is diamond, but the energy gap is very large for it to become a semiconductor.

In an insulator, the energy gap is large enough to prevent the valence electrons to be excited to the conduction band. However, if the applied electric field is greater than a critical value (known as the critical field), such that the valence electrons gain energy that is equal to or greater than the energy gap, they can be excited to the conduction band. In such cases, the insulator behaves like a good conductor as long as the applied electric field is greater than the critical field. Thus, insulators, which have large energy gaps, are used as breaking devices in high-voltage transmission. When the external electric field is greater than the critical field required to cross the energy gap, there is good transmission of electric current because the insulator behaves as a good conductor, but when the applied electric field drops below the critical value, the insulator stops the flow of current. The transmission of electricity is restored by appropriate repairs such that the external electric field is again larger than the critical field.

In case of intrinsic semiconductors (pure semiconductors are called intrinsic in order to distinguish them from impurity [or doped] semiconductors), the energy gap between the valence band and the conduction band is sufficiently low (0.7 eV for Ge and 1.09 eV for Si). Although an intrinsic semiconductor behaves as an insulator at absolute zero temperature, some valence electrons are thermally excited to the conduction band, leaving behind an equal number of unoccupied states (holes) in the valence band. We will later show that these holes act like positive charges. In an applied electric field, both the (few) electrons in the conduction band and the holes in the valence band are excited and move in opposite directions, thereby conducting electricity. However, because

the number of conducting electrons and holes is much smaller than that compared to metals, the resistivity of semiconductors is very large compared to that of metals. When the temperature is increased, more valence electrons are excited into the conduction band, leaving behind more (positively charged) holes in the valence band. Thus, the resistivity of semiconductors decreases with increase of temperature because of the increase in the number of carriers. In contrast, the resistivity of metals increases with the increase of temperature because the electrons are scattered by the lattice ions (phonons) and lattice impurities due to thermal vibrations.

We will now discuss the typical case of the most commonly used semiconductors such as Si ($1s^2 2s^2 2p^6 3s^2 3p^2$) and Ge ($1s^2 2s^2 2p^6 3s^2 3p^6 3d^{10} 4s^2 4p^2$). We note that Si has two $3s$ and two $3p$ electrons, and Ge has two $4s$ and two $4p$ electrons. Normally, we would expect Si and Ge to be conductors because each one of them has four unfilled p states. However, the $3s$ and $3p$ levels (for Si) and the $4s$ and $4p$ levels (for Ge) mix when they form covalent bonds. The energy of the electron levels corresponding to the four space-symmetric wave functions, one for the $2s$ levels and three for the $2p$ levels, is lowered. The energy of the other four levels, one $2s$ and three $2p$, is raised. Thus, the valence band has four levels per atom that are filled, whereas the conduction band is empty.

An interesting example is Sn, which is also a tetravalent solid. It has two phases: in one phase it is metallic, whereas in another phase it is a semiconductor. The shape of the Brillouin zone changes when the crystal structure is changed, and hence, it becomes possible to have large energy gaps to hold all the electrons. On the other hand, Pb, which is a tetravalent solid is a metal because of the band structure such that the electrons in the conduction band can be excited to higher energy states by an electric field. To summarize, the elements in Group IV of the periodic table have a wide range of properties. C in the form of a diamond is an insulator, Si and Ge are semiconductors, Sn can either be a metal or a semiconductor, whereas Pb is a metal.

The pentavalent solids such as As, Sb, and Bi have 5 electrons per atom. However, their crystal structure is such that there are 2 atoms per unit cell. Thus, there are 10 electrons per unit cell. These 10 electrons would normally fill 5 bands. However, due to the effect of the band structure, the fifth band is not quite full because there is a little overlap (schematically very similar to Figure 4.12a) with the sixth band. Therefore, even at zero temperature, a few electrons in both the fifth and the sixth bands are always available to be excited (to carry the current) when an external electric field is applied. These are poor conductors and are known as *semimetals.*

The iron group of the transition metals (Cr, Mn, Fe, Co, Ni) and the groups that are higher in the periodic table have incomplete d-shells. For example, only 6 out of the 10 states in the $3d$-shell of Fe atom are filled, while two more electrons fill the outer $4s$ state. The d-orbitals in a solid overlap to form a "d-band" that can be treated by a tight-binding or LCAO method (see Chapter 5). The two electrons that form an s-band (in some transition metals there are electrons in both s and p states, and the corresponding band is known as the *s-p-band*) hybridize with the narrow d-band that is capable of accommodating up to 10 electrons per atom. This hybridization between d-bands and s-bands is shown in Figure 4.13. These bands are called resonance bands, and the hybridization is important in understanding the magnetic phenomena. Because neither of the bands is full, these solids are metallic and the conduction is mainly metallic.

The four possible band structures for a solid are shown in Figure 4.14. Thus, it is possible to explain the occurrence of metals (good conductors), semimetals (poor conductors), insulators, and (intrinsic) semiconductors from a simple one-dimensional picture of band theory. We will later discuss in detail the characteristic properties of each of these solids.

We have summarized, by using the one-dimensional band theory of solids, the classification of solids into metals (good conductors), semimetals (poor conductors), insulators, and semiconductors. The rule of thumb is that each Brillouin zone has room for two electrons per primitive cell of a sample. If we consider a linear lattice that has one monovalent atom per primitive cell, the Brillouin zone is half filled. The electrons near the Fermi surface (the surface that separates the highest filled-energy states from the empty states) can be accelerated by an applied electric field, and because there are many empty states available, the metal is a good conductor. If there is one divalent atom per primitive cell, the first zone should be normally filled with electrons. However, in a three-dimensional band picture, there is usually overlap between the top of the electron states in the first zone and the bottom of the empty electron states in the second zone. The energy gap (in different k directions) disappears. This leads the electrons to spill over from the top of the first zone to the bottom of the second zone, and the Fermi surface is in both zones. Such metals are not very good metals because of the small number of electrons that are excited in an external electric field. If the atom in each lattice point is trivalent, the first Brillouin zone is completely filled, but the second zone is half full.

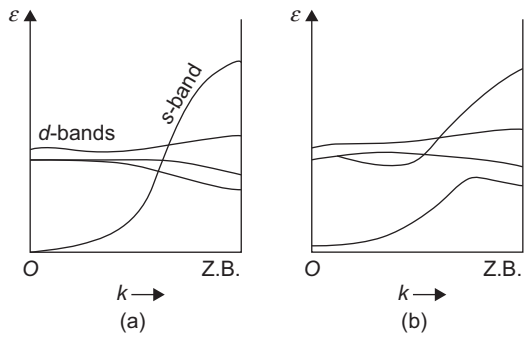

FIGURE 4.13

(a) *d*-bands crossing *s*-bands; (b) *s-d* hybridization.

The Fermi surface is in the second zone, and because a large number of electron states above the Fermi surface are empty, the solid is a metal and a good conductor. If there is a quadrivalent atom per primitive cell, the solid is either an insulator or a semiconductor depending on the magnitude of the energy gap. If there are two quadrivalent atoms per primitive cell (examples

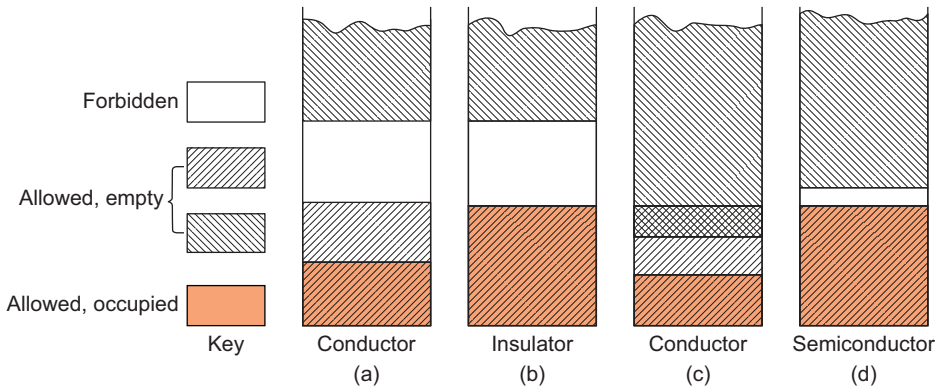

FIGURE 4.14

Four possible band structures for a solid: (a) conductor because the band is partially full, (b) insulator because of large energy gap between the filled and the empty bands, (c) semimetals because the allowed bands overlap, and (d) semiconductor because of the very small energy gap between the filled and the empty bands.

are diamond, silicon, and germanium), there are eight valence electrons per primitive cell. Because the bands do not overlap, diamond is an insulator (because of the large energy gap), and both silicon and germanium are intrinsic semiconductors because of the small energy gap. In both cases, there is no Fermi surface in the usual sense, but for semiconductors, the Fermi level is usually located at the center of the energy gap.

The electrons in metals in the highest occupied states have immediate access to the empty states, and the surface that separates these states is called the Fermi surface. However, the highest occupied electron states in insulators and semiconductors (at zero temperature) are separated from each other by energy gaps. Thus, the Fermi surface plays a vital role in determining the properties of metals. The Fermi surface of free electrons is a sphere in three dimensions. However, the Fermi surface is much more complex in a metal because of the periodic potential. To be able to understand the increasing complexity of the Fermi surface in such solids, we need to first understand the properties of two- and three-dimensional lattices and the Brillouin zones. In the nearly free electron approximation, a constant-energy surface is perpendicular to a Bragg plane when they intersect.

4.11 BRILLOUIN ZONES

We will first discuss the Brillouin zones for a two-dimensional square lattice, which we discussed in Chapter 1. The Bragg planes bisect the line joining the origin to points of the reciprocal lattice. The first Brillouin zone is defined as the set of points reached from the origin without crossing any Bragg plane (except that the points lying on the Bragg planes are common to two or more zones). The second Brillouin zone is the set of points that can be reached from the first zone by crossing only one Bragg plane. One can make a generalization of this definition and define the nth Brillouin zone as the set of points that can be reached from the origin by crossing no fewer than $n - 1$ Bragg planes. The first four zones of the two-dimensional square Bravais lattice are shown in Figure 4.15.

In general, a Brillouin zone can be constructed by using the rule that an incoming wave scatters strongly off a lattice with reciprocal lattice vector $\mathbf{K}$, only when

$$\mathbf{k} \cdot \mathbf{K} = \tfrac{1}{2}K^2. \tag{4.102}$$

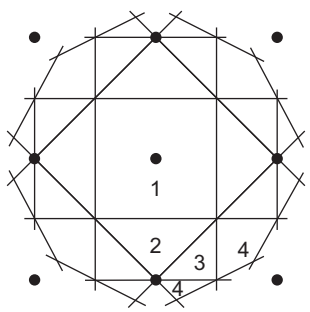

FIGURE 4.15

Brillouin zones for a two-dimensional square Bravais lattice. The first three zones are contained entirely in the square.

The set of points that satisfy Eq. (4.102) is a plane that is perpendicular to the vector connecting the origin to $\mathbf{K}$ and lying midway between 0 and $\mathbf{K}$. When many such planes are constructed using all possible $\mathbf{K}$ values, the origin would be enclosed within a solid region. This is the first Brillouin zone because all points inside are closer to the origin than any reciprocal lattice vector. An example of this construction is the Brillouin zone of a two-dimensional centered rectangular lattice shown in Figure 4.16.

As explained earlier, the nth Brillouin zone is constituted of the set of points in reciprocal space that is closer to the $n-1$ reciprocal points

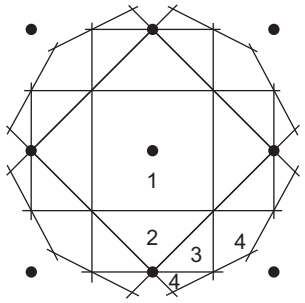

FIGURE 4.16

The zone boundaries for a two-dimensional centered rectangular lattice are obtained by drawing perpendicular bisectors between the origin and the nearby reciprocal points.

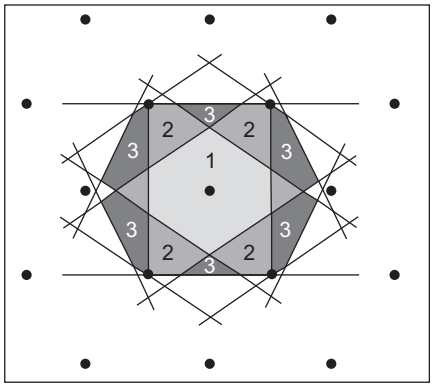

FIGURE 4.17

The first three Brillouin zones of a two-dimensional centered rectangular lattice.

than it is to the origin. The construction of the first three Brillouin zones for a rectangular centered lattice is obviously more complicated than a square lattice. Such construction for the first three Brillouin zones, shaded in different ways, is shown in Figure 4.17.

The first zone is the set of points closer to the origin than any other reciprocal lattice point. The second zone is constituted of the set of points that one reaches by crossing only one zone boundary. The third zone is the set of points that one reaches by crossing a minimum of two zone boundaries.

The construction of Brillouin zones for a three-dimensional lattice gets more complicated. For example, the first Brillouin zone of a simple cubic lattice is simple cubic, but the first Brillouin zones of a bcc and a fcc lattice are much more complicated. The first Brillouin zone of a simple cubic lattice with the symmetry points is shown in Figure 4.18. (The symmetry points are explained in Appendix A.)

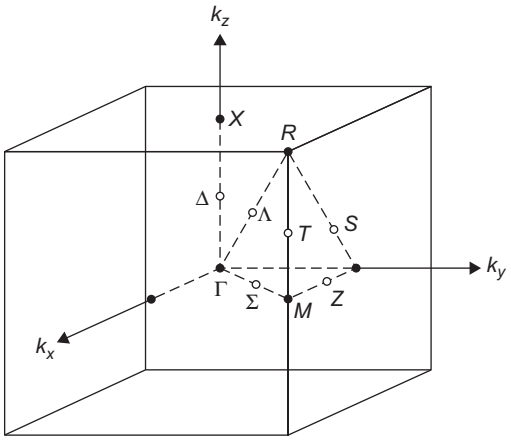

FIGURE 4.18

First Brillouin zone of the simple cubic lattice.

In Figure 4.18, the point Γ is at the center of the zone. *R* is at the corner of the cube that is connected to the other corners so that all eight corners are a single point. Γ and *R* have the same representation, the cubic group. *X* is at the intersection of the k_z axis with the lower face of the cube. *M* is at the intersection of the k_xk_y plane with the vertical edges (there are three equivalent points to *M*). *M* and *X* have the same symmetry elements 4/mmm. *T* is equivalent to the three points on the other vertical edges. The points *T* and Δ have the same point group, 4mm. The point Λ has point group 3m. The points Σ and *S* are holomorphic to 2mm. The point *Z* has two mirror planes and a two-fold axis.

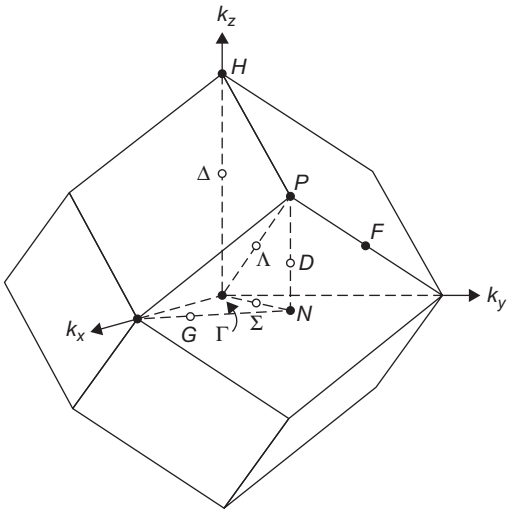

FIGURE 4.19

The first Brillouin zone of the bcc lattice.

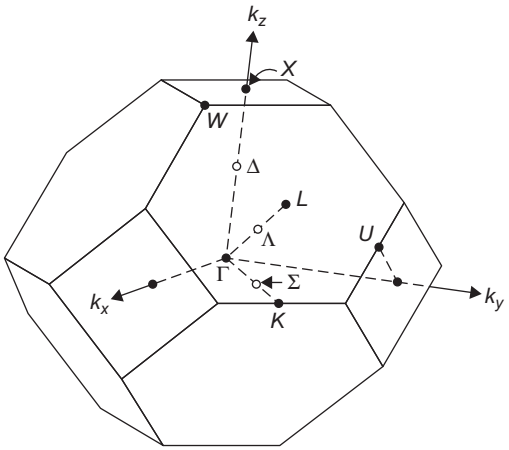

FIGURE 4.20

The Brillouin zone of the fcc lattice showing the symmetry points.

The first Brillouin zone of the body-centered cubic lattice, which is a rhombic dodecahedron, is shown in Figure 4.19 along with the symmetry points and the axes.

The symmetry operations of $\Gamma, \Delta, \Lambda, \Sigma$ are the same as the similar points in the simple cubic lattice shown in Figure 4.19. H has the full cubic symmetry like Γ.

The Brillouin zone of a face-centered cubic lattice is a truncated octahedron that is shown in Figure 4.20. Here, Γ is at the center of the zone, L is at the center of each hexagonal face, X is at the center of each square face, and W is at each corner formed from one square and two hexagons.

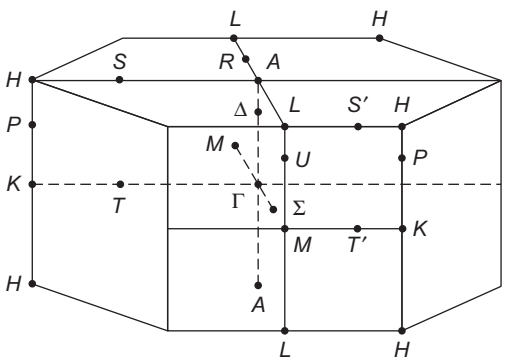

FIGURE 4.21

The Brillouin zone of the hcp structure.

The Brillouin zone of the hexagonal close-packed structure is shown with the symmetry points in Figure 4.21.

4.12 FERMI SURFACE

4.12.1 Fermi Surface (in Two Dimensions)

For free electrons, the Fermi surface is a circle in two dimensions and a sphere in three dimensions. The two-dimensional Fermi circles corresponding to one, two, and three electrons per atom for a square lattice are shown in Figure 4.22.

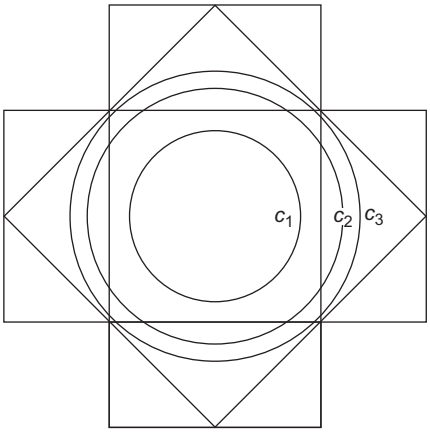

FIGURE 4.22

Two-dimensional Fermi circles corresponding to one, two, and three electrons per atom in the Brillouin zones of a square lattice (without distortion at the zone boundaries).

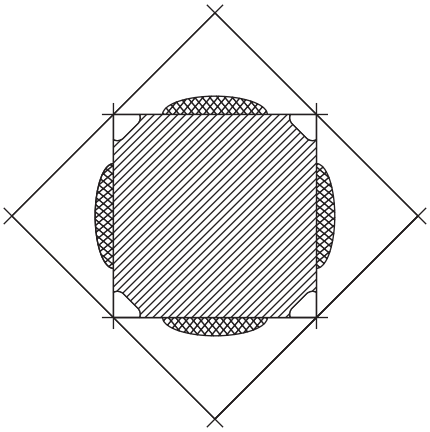

FIGURE 4.23

The distortion of the Fermi circle of a two-dimensional electron gas due to a periodic potential.

The weak periodic potential causes a distortion of the Fermi circle of a two-dimensional electron gas as it approaches the zone boundary. For example, in Figure 4.22, the free electron circle c_1 is entirely within the first Brillouin zone. However, the free electron circles c_2 and c_3 intersect the zone boundaries. Because there is an energy gap between the electron states in the zone boundaries, the Fermi circle is distorted as it approaches the zone boundaries. In addition, the energy curves must be normal to the zone boundaries and develop "necks." The distortion of the Fermi circle by the weak periodic potential is shown in Figure 4.23.

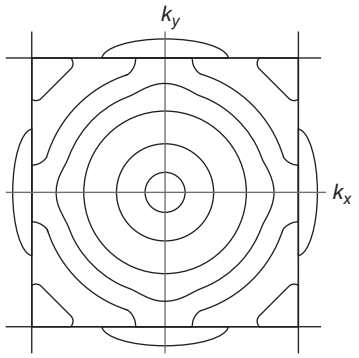

FIGURE 4.24

Distortion of the free electron Fermi circles as energy contours approach the zone boundaries.

However, the distortion of the Fermi circle does not suddenly develop only when the circle approaches the Brillouin zone boundary. The energy contours develop bumps that increase as they approach the zone boundary. The free electron Fermi circles are distorted much before they approach the zone boundary and develop "necks" at the zone boundary because of the energy gap. The distortion of these energy contours is shown in Figure 4.24.

We note from Figure 4.24 that there is a decrease in the constant energy contour when the Fermi circle has contact with the Brillouin zone.

4.12.2 Fermi Surface (in Three Dimensions)

The occupied states of the free electron gas lie within a sphere. The radius of this sphere is the Fermi radius, and the surface is the Fermi surface. In Figure 4.25a, it is shown that when $V_{\mathbf{K}} = 0$, the free electron Fermi sphere meets the zone boundary at a distance ½**K** from the origin O, but there is no distortion of the Fermi surface. In Figure 4.25b, $V_{\mathrm{K}} \neq 0$ and there is distortion of the Fermi sphere at the zone boundary. The Fermi surface intersects the plane in two circles.

It can be shown (Problem 4.6) that the radii r_1 and r_2 of these circles are related by the equation

$$(r_1{}^2 - r_2{}^2) = \frac{4m}{\hbar^2} |V_{\mathbf{K}}| . \tag{4.103}$$

In Figure 4.26, we show a free electron Fermi surface completely enclosing the first Brillouin zone of a two-dimensional centered rectangular lattice. We note that the shape of the Fermi surface is modified near the zone boundaries.

Figure 4.27 shows the portion of the Fermi surface in the second Brillouin zone that is mapped back into the first zone so that the energy surface is continuous. This is essentially achieved by using the reduced zone scheme. The portion of the Fermi surface is mapped back to the first Brillouin zone by appropriate translations through reciprocal lattice vectors so that the energy surface is contiguous, as shown in Figure 4.27. However, this method of mapping back the Fermi surface to the first Brillouin zone by any single reciprocal lattice vector becomes increasingly complicated even when there are electron states in the third Brillouin zone. In that case, it is not possible to map the contiguous portions of the third Brillouin zone into the first Brillouin zone by a single reciprocal lattice vector. In such cases, Harrison's method of construction of the Fermi surface becomes very useful.

4.12.3 Harrison's Method of Construction of the Fermi Surface

When the band structure of a solid gets more complicated and the number of valence electrons per atom is large, it becomes very difficult to draw the Fermi surface of a metal. As we have noted, the shape and contours of the Fermi surface are important in determining the physical properties of a metal. To make this task simpler, Harrison[2] proposed a method of constructing the Fermi surface of

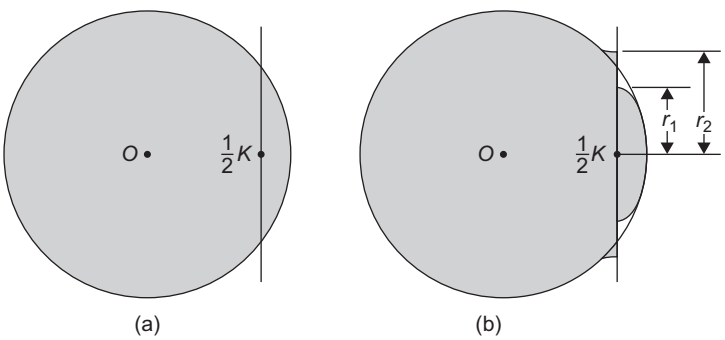

FIGURE 4.25

(a) Free electron sphere cutting Bragg plane when $V_{\mathbf{K}} = 0$; (b) free electron sphere cutting Bragg plane when $V_{\mathbf{K}} \neq 0$.

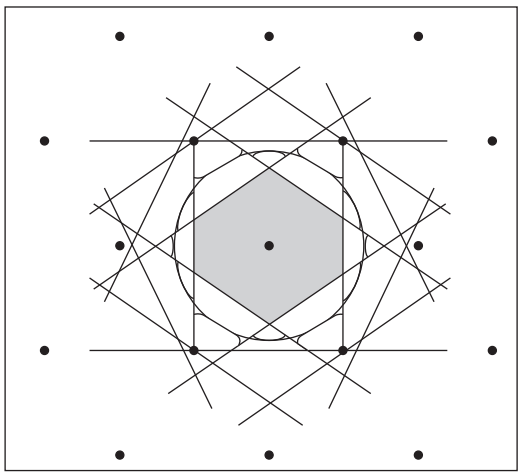

FIGURE 4.26

Free electron Fermi surface completely enclosing the Brillouin zone of a two-dimensional centered rectangular lattice.

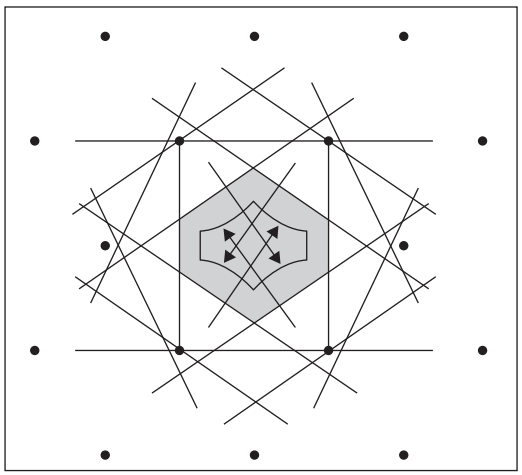

FIGURE 4.27

The portion of the Fermi surface in the second Brillouin zone mapped back to the first zone.

a metal of valence Z by using the periodic zone scheme. According to his method, if the perturbing potential is very small, the energy surfaces must be spheres. The radius of the sphere, which contains ½Z times the volume of a zone (there are two electrons per each $\mathbf{k}$ state because of spin), is drawn with the center at the origin. The same sphere is drawn about each point of the reciprocal lattice, and one obtains a pattern that has the periodicity of the repeated zone scheme. Harrison's construction of the free electron Fermi surface is shown in Figure 4.28.

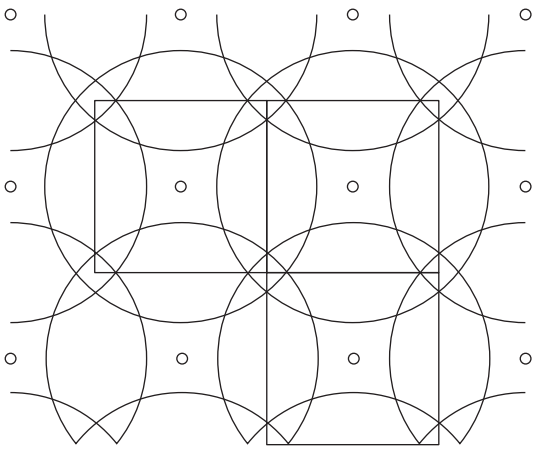

FIGURE 4.28

Free electron Fermi surface constructed by using Harrison's method.

From Figure 4.28, one can choose various parts that are continuously fitted together such that the surfaces are repeated in each zone. These different figures are either a branch of the Fermi surface or a part of the Fermi surface in the second and the third zone. The first zone is completely filled and therefore does not have a Fermi surface. The different parts of the Fermi surface for the second and the third zones are shown in Figures 4.29a and b.

We note from Figures 4.29a and b that these surfaces have cusps where the parts join because they are drawn for spherical Fermi surfaces (free electrons). However, in the nearly free electron model, the Fourier components of the potential would round off the corners, and one would obtain smooth

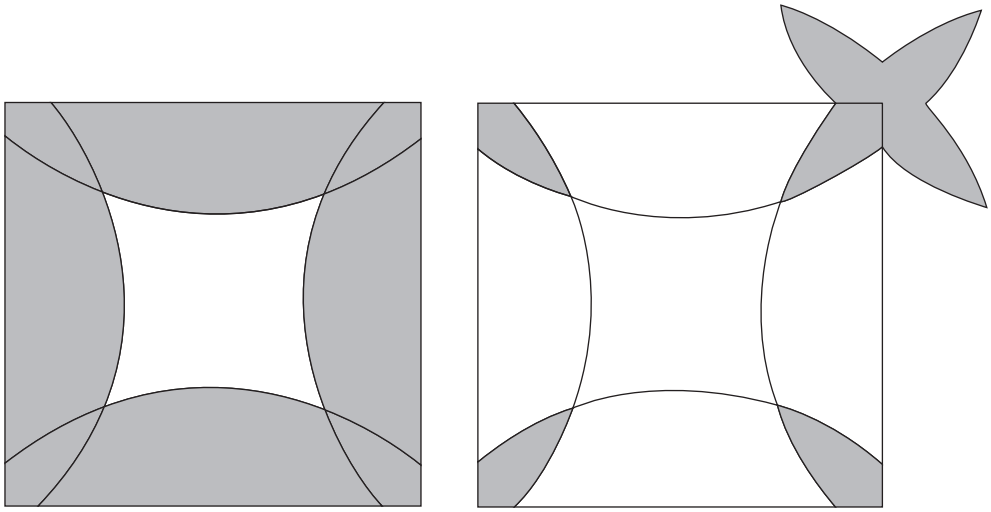

FIGURE 4.29

(a) Fermi surface of the second zone in the reduced zone obtained from Harrison's construction (Figure 4.28). The orbit is a hole orbit. (b) Fermi surfaces in the third Brillouin zone. The orbit in the top-right corner (rosettes) is in the reduced zone scheme.

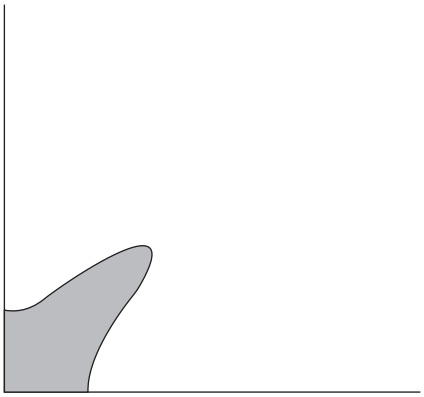

FIGURE 4.30

One corner of the third zone of Figure 4.29b due to the effect of the periodic potential.

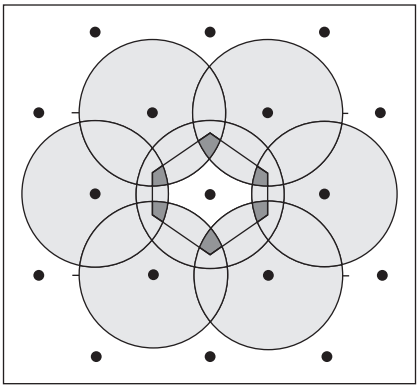

FIGURE 4.31

The Harrison construction of the Fermi surfaces for a two-dimensional centered rectangular lattice.

geometrical objects. This rounding off of the corners and the fact that the line of constant energy intersects the zone boundary at normal incidence are shown for a corner of the third zone in Figure 4.30.

A more visual construction of Harrison's method (see Figure 4.31) shows how the surface in the nth Brillouin zone looks when it is mapped into the first Brillouin zone (i.e., the reduced zone scheme).

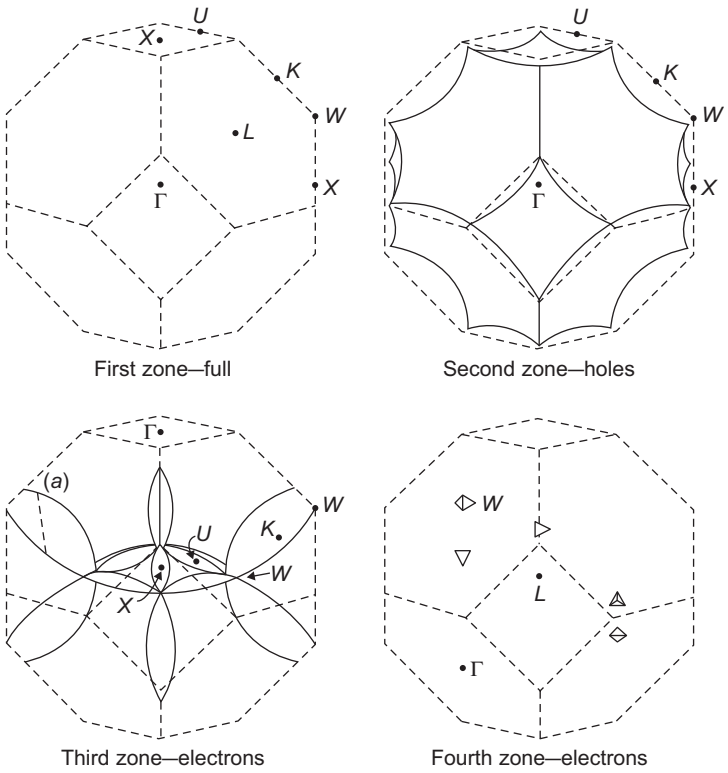

FIGURE 4.32

Free electron Fermi surface of aluminum in the reduced zone scheme obtained by Harrison.

Reproduced from Harrison[2] with the permission of the American Physical Society.

Figure 4.31 shows how the surface of the nth Brillouin zone looks when it is mapped back into the first Brillouin zone. The Fermi sphere in the second Brillouin zone is identified by all points in the first Brillouin zone that are inside two or more spheres. The Fermi sphere in the third Brillouin zone is identified by all points in the first Brillouin zone that are inside three or more spheres. One can extend this method of obtaining Fermi surfaces in three dimensions by using the operations of constructive solid geometry. The free electron Fermi surface of aluminum in the reduced zone scheme, as obtained by Harrison, is shown in Figure 4.32.

PROBLEMS

4.1. It can be shown in quantum mechanics that the momentum operator is the generator of infinitesimal translations ε (equivalent to an analogous relation in classical mechanics)

$$\hat{T}(\varepsilon) = 1 - \frac{i\varepsilon}{\hbar}\hat{p}. \tag{1}$$

Using $\varepsilon = a/N$ in Eq. (1), one obtains

$$\hat{T}(a/N) = 1 - \frac{ia}{\hbar N}\hat{p}. \tag{2}$$

By using the formula

$$e^{-ax} = \lim_{N\to\infty}(1 - \tfrac{ax}{N})^N, \tag{3}$$

show that the operator $\hat{T}(a)$ corresponding to a finite translation a (in one dimension) can be obtained by

$$\hat{T}(a) = \lim_{N\to\infty}[\hat{T}(a/N)]^N = e^{-ia\hat{p}/\hbar}. \tag{4}$$

4.2. In general, any function $f(\mathbf{r})$ can be expanded in terms of the plane waves that form a complete set of functions. However, if a function $f(\mathbf{r}) = f(\mathbf{r}+\mathbf{R})$ for all $\mathbf{r}$ and all $\mathbf{k}$ in the Bravais lattice, then it is easy to show that

$$f(\mathbf{r}) = \sum_{\mathbf{K}} f_{\mathbf{K}} e^{i\mathbf{K}\cdot\mathbf{r}} \tag{1}$$

because only $e^{i\mathbf{K}\cdot\mathbf{r}}$ has the periodicity of the lattice. Show that the Fourier coefficients $f_{\mathbf{K}}$ are given by

$$f_{\mathbf{K}} = \frac{1}{v}\int_C d\mathbf{r}\, e^{-i\mathbf{K}\cdot\mathbf{r}} f(\mathbf{r}), \tag{2}$$

where v is the volume of the primitive cell C. To prove Eq. (2), first show that

$$\int_C d\mathbf{r} e^{i\mathbf{K}\cdot(\mathbf{r}+\mathbf{l})} = \int_{C'} d\mathbf{r} e^{i\mathbf{K}\cdot\mathbf{r}} = \int_C d\mathbf{r} e^{i\mathbf{K}\cdot\mathbf{r}}, \tag{3}$$

where C' is the translated cell when C is translated through a vector $\mathbf{l}$. From Eq. (3), one obtains

$$(e^{i\mathbf{K}\cdot\mathbf{l}} - 1)\int_C d\mathbf{r}\, e^{i\mathbf{K}\cdot\mathbf{r}} = 0, \tag{4}$$

from which it follows that (because $e^{i\mathbf{K}\cdot\mathbf{l}} \neq 1$)

$$\int_C d\mathbf{r}\, e^{i\mathbf{K}\cdot\mathbf{r}} = 0, \tag{5}$$

which is needed to prove Eq. (2) from Eq. (1).

4.3. By using the Born–von Karman boundary conditions, one obtains the periodicity for a crystal lattice (which can be considered as a very large Bravais lattice with the volume of the primitive cell V, the volume of the crystal),

$$f(\mathbf{r}) = f(\mathbf{r} + M_i\mathbf{a}_i),\ i = 1, 2, 3. \tag{1}$$

It has been shown that a vector of the reciprocal to this lattice has the form

$$\mathbf{k} = \sum_{i=1}^{3}\frac{m_i}{M_i}\mathbf{b}_i. \tag{2}$$

In a manner similar to Problem 4.2, show that if

$$f(\mathbf{r}) = \sum_{\mathbf{k}} f_{\mathbf{k}} e^{i\mathbf{k}\cdot\mathbf{r}}, \tag{3}$$

then

$$\int_V d\mathbf{r}\, e^{i\mathbf{k}\cdot\mathbf{r}} = 0, \tag{4}$$

and

$$f_{\mathbf{k}} = \frac{1}{V}\int d\mathbf{r} e^{-i\mathbf{k}\cdot\mathbf{r}} f(\mathbf{r}). \tag{5}$$

4.4. It was shown in Eq. (4.4) that the lattice potential $V(\mathbf{r})$ has the periodicity of the lattice,

$$V(\mathbf{r}) = V(\mathbf{r}+\mathbf{R}). \tag{1}$$

Therefore, using the results from Problem 4.2, one obtains

$$V(\mathbf{r}) = \sum_{\mathbf{K}} V(\mathbf{K}) e^{i\mathbf{K}\cdot\mathbf{r}}. \tag{2}$$

From Eq. (2) of Problem 4.2, one obtains

$$\mathrm{V}(\mathbf{K}) = \frac{1}{v}\int_C d\mathbf{r}\, e^{-i\mathbf{K}\cdot\mathbf{r}} V(\mathbf{r})\cdot \tag{3}$$

Assume that $V(0) = 0$. Show that because $V(\mathbf{r})$ is real and if the crystal has inversion symmetry,

$$V(\mathbf{K}) = V(-\mathbf{K}) = V(\mathbf{K})^*. \tag{4}$$

Because the wave function $\psi(\mathbf{r})$ can be expanded in the set of plane waves

$$\psi(\mathbf{r}) = \sum_{\mathbf{q}} C_{\mathbf{q}} e^{i\mathbf{q}\cdot\mathbf{r}}, \tag{5}$$

where the $\mathbf{q}'s$ are wave vectors of the form $\mathbf{q} = \sum_{i=1}^{3} \frac{m_i}{M_i}\mathbf{b}_i$, show that the Schrodinger equation can be written as

$$\left(-\frac{\hbar^2}{2m}\nabla^2 + V(\mathbf{r}) - E\right)\psi(\mathbf{r}) = \sum_{\mathbf{q}} \left\{\left(\frac{\hbar^2}{2m}q^2 - E\right)C_{\mathbf{q}} + \sum_{\mathbf{K}'} V_{\mathbf{K}'} C_{\mathbf{q}-\mathbf{K}'}\right\} e^{i\mathbf{q}\cdot\mathbf{r}} = 0. \tag{6}$$

The coefficient of each term in Eq. (6) must vanish (because the plane waves are orthogonal),

$$\left(\frac{\hbar^2}{2m}q^2 - E\right)C_{\mathbf{q}} + \sum_{\mathbf{K}'} V_{\mathbf{K}'} C_{\mathbf{q}-\mathbf{K}'} = 0. \tag{7}$$

If $\mathbf{q} = \mathbf{k} - \mathbf{K}$, where $\mathbf{k}$ lies in the first Brillouin zone and changing the variables to $\mathbf{K}' \rightarrow \mathbf{K}' - \mathbf{K}$, show that Eq. (7) can be written as

$$\left(\frac{\hbar^2}{2m}(\mathbf{k}-\mathbf{K})^2 - E)C_{\mathbf{k}-\mathbf{K}}\right) + \sum_{\mathbf{K}'} V_{\mathbf{K}'-\mathbf{K}} C_{\mathbf{k}-\mathbf{K}'} = 0. \tag{8}$$

Eq. (8) shows that for a fixed $\mathbf{k}$ in the first Brillouin zone, only wave vectors that differ from $\mathbf{k}$ by a reciprocal lattice vector are coupled. Rewriting $\psi(\mathbf{r})$ as $\psi_{\mathbf{K}}(\mathbf{r})$ and E as ε, from Eqs. (5) and (8), show that

$$\psi_{\mathbf{k}}(\mathbf{r}) = e^{i\mathbf{k}\cdot\mathbf{r}}\left(\sum_{\mathbf{G}} C_{\mathbf{k}-\mathbf{K}} e^{-i\mathbf{K},\mathbf{r}}\right), \tag{9}$$

and

$$\left(\frac{\hbar^2}{2m}(\mathbf{k}-\mathbf{K})^2 - \varepsilon\right) C_{\mathbf{k}-\mathbf{K}} + \sum_{\mathbf{K}'} V_{\mathbf{K}'-\mathbf{K}} C_{\mathbf{k}-\mathbf{K}'} = 0. \tag{10}$$

Define

$$u_k(\mathbf{r}) = \sum_{\mathbf{K}} C_{\mathbf{k}-\mathbf{K}} e^{-i\mathbf{K}\cdot\mathbf{r}}, \tag{11}$$

and hence show from Eqs. (9) and (11) that

$$\psi_{\mathbf{k}}(\mathbf{r}) = e^{i\mathbf{k}\cdot\mathbf{r}} u_{\mathbf{k}}(\mathbf{r}). \tag{12}$$

From Eq. (11), show that

$$u_{\mathbf{k}}(\mathbf{r}+\mathbf{R}) = u_{\mathbf{k}}(\mathbf{r}). \tag{13}$$

Here, $\psi_{\mathbf{k}}(\mathbf{r})$ is the Bloch function, and $u_{\mathbf{k}}(\mathbf{r})$ is the periodic part of the Bloch function (in three dimensions).

4.5. In the Kronig–Penney model, an electron in a one-dimensional lattice is in the presence of a potential

$$V(x) = \sum_n V_0 \phi(x-nb)\varphi(nb+c-x), \tag{1}$$

where $b > c$, n is zero or a positive integer, $b + c = L$ and φ is the Heaviside unit-step function

$$\varphi(x) = \left\{ \begin{array}{ll} 0, & x<0. \\ 1, & x>0. \end{array} \right\}. \tag{2}$$

The one-dimensional periodic potential can be represented as

$$V(x+L) = V(x), \tag{3}$$

as shown in Figure P4.1. The potential energy as a function of distance is given in Figure P4.1 Because there is symmetry under the displacement by L, it can be shown that the eigenfunction is

$$\psi(x) = e^{ikx} u(x), \tag{4}$$

where $u(x+L) = u(x)$ and k is arbitrary, and as we will show, it is the propagation constant. In addition, we consider the one-dimensional periodic potential visualized as a ring of circumference NL, such that

$$\psi(x+NL) = \psi(x). \tag{5}$$

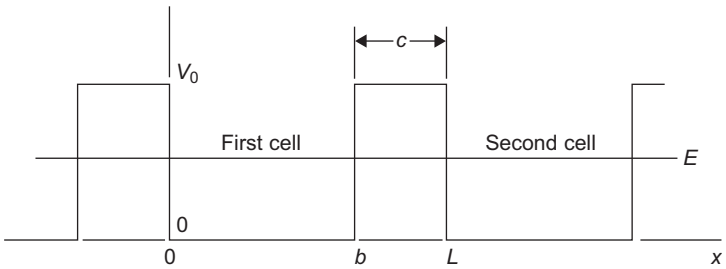

FIGURE P4.1

The Kronig–Penny model of the square potential lattice.

From Eqs. (4) and (5), we obtain

$$e^{ik(x+NL)} = e^{ikx}, \tag{6}$$

from which, we obtain

$$k = \frac{2\pi n}{NL}, \text{ where } n = 0, \pm 1, \pm 2, \ldots. \tag{7}$$

Here, k is called the propagation constant of the state. We represent the wave function as

$$\begin{aligned} \psi(x+L) &= e^{ikL}\psi(x), \\ \psi(x) &= e^{ikx}u(x), \end{aligned} \tag{8}$$

where

$$u(x+L) = u(x). \tag{9}$$

The advantage of Eq. (8) is that if we know $\psi(x)$ for any one cell of the periodic lattice, it can be calculated for any other cell.

To solve this problem, one can use the one-dimensional equivalence of Eq. (4.35) (except that k is now called the propagation constant of the state $k = \frac{2\pi n}{NL}$),

$$\frac{d^2u}{dx^2} + 2ik\frac{du}{dx} + \frac{2m}{\hbar^2}\left[E - V(x) - \frac{\hbar^2k^2}{2m}\right]u(x) = 0. \tag{10}$$

From Figure P4.1 and Eq. (9), we have the periodicity condition

$$u(x+L) = u(x) \text{ and } du(x+L)/dx = du(x)/dx. \tag{11}$$

Introducing the notations

$$k_1 = \left(\frac{2mE}{\hbar^2}\right)^{\frac{1}{2}} \text{ and } k_2 = \left[\frac{2m}{\hbar^2}(V_0 - E)\right]^{\frac{1}{2}}, \tag{12}$$

the solution of Eq. (10) for the square lattice can be written as

$$u_1(x) = A\,e^{i(k_1-k)x} + Be^{-i(k_1+k)x}, \tag{13}$$

for the region of the well (from $x = 0$ to $x = b$), and

$$u_2(x) = Ce^{(k_2-ik)x} + De^{-(k_2+ik)x}, \tag{14}$$

for the region of the hill ($x = b$ to $x = L$). Using the periodicity conditions mentioned previously, show that

$$A + B = e^{-ikL}[Ce^{k_2 L} + De^{-k_2 L}], \tag{15}$$

and

$$ik_1(A - B) = k_2 e^{-ikL}[Ce^{k_2 L} - De^{-k_2 L}]. \tag{16}$$

Show from the continuity conditions that

$$Ae^{ik_1 b} + Be^{-ik_1 b} = Ce^{k_2 b} + De^{-k_2 b}, \tag{17}$$

and

$$ik_1[Ae^{ik_1 b} - Be^{-ik_1 b}] = k_2[Ce^{k_2 b} - De^{-k_2 b}]. \tag{18}$$

Eqs. (15) through (18) have nontrivial solutions only if the determinant of the matrix of the coefficients vanishes. Show that

$$\cos k_1 b \cosh k_2 c - \frac{k_1^2 - k_2^2}{2k_1 k_2} \sin k_1 b \sinh k_2 c = \cos kL, \quad E < V_0. \tag{19}$$

It can also be shown that

$$\cos k_1 b \cos k_2 c - \frac{k_1^2 + k_2^2}{2k_1 k_2} \sin k_1 b \sin k_2 c = \cos kL, \quad E > V_0. \tag{20}$$

Eqs. (19) and (20) can be solved numerically, and the results are shown in Figure P4.2. The remarkable feature is that the right sides of the eigenvalue equations are bound between –1 and +1. Thus, only those values of E that make the left side of these equations also lie in the same interval and all other values are excluded. This is the origin of the band structure in solids.

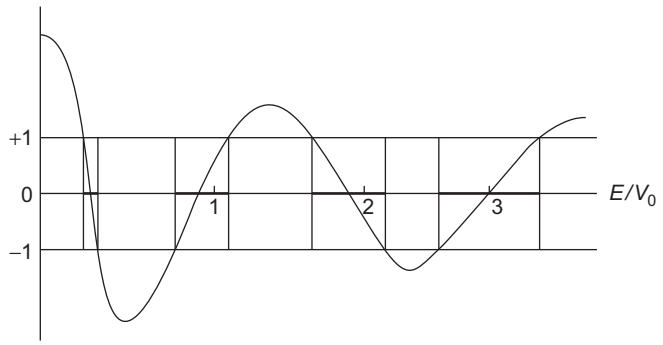

FIGURE P4.2

The left sides of Eqs. (19) and (20) are plotted as functions of E that join smoothly at $E = V_0$. The heavy lines display the allowed range of energy values.

4.6. If we write

$$\mathbf{k} = \tfrac{1}{2}\mathbf{K} + \mathbf{q},$$

Eq. (4.82) can be rewritten as

$$\varepsilon(\mathbf{k}) = \varepsilon^0_{\mathbf{K}/2} + \frac{\hbar^2 q^2}{2m} \pm \left(4\varepsilon^0_{\mathbf{K}/2}\frac{\hbar^2 q_\parallel^2}{2m} + |V_{\mathbf{K}}|^2\right)^{\frac{1}{2}}, \tag{1}$$

where $q_\parallel$ is the parallel component of $\mathbf{q}$. We can also write

$$\varepsilon_F = \varepsilon^0_{\mathbf{K}/2} - |V_{\mathbf{K}}| + \delta. \tag{2}$$

Show that:

a. When $\delta < 0$, no Fermi surface intersects the Bragg plane.

b. When $0 < \delta < 2|V_{\mathbf{K}}|$, the Fermi surface intersects the Bragg plane in a circle of radius,

$$r = \sqrt{\frac{2m\delta}{\hbar^2}}. \tag{3}$$

c. When $\delta > |2V_{\mathbf{K}}|$, the Fermi surface cuts the Bragg plane in two circles (because it lies in both bands) of radii r_1 and r_2 and

$$r_1{}^2 - r_2{}^2 = \frac{4m\,|V_{\mathbf{K}}|}{\hbar^2}. \tag{4}$$

References

1. Ashcroft NW, Mermin ND. *Solid state physics*. Toronto: Thomson Learning; 1976.
2. Harrison WA. Band structure of aluminum. *Phys Rev* 1960;**118**:1182.
3. Harrison WA. *Solid state theory*. New York: McGraw-Hill; 1969.
4. Kittel C. *Introduction to solid state physics*. New York: John Wiley & Sons; 1976.
5. Liboff RI. *Introductory quantum mechanics*. Reading, MA: Addison-Wesley; 1980.
6. Madelung O. *Introduction to solid state theory*. New York: Springer-Verlag; 1978.
7. Marder MP. *Condensed matter physics*. New York: John Wiley & Sons; 2000.
8. Myers HP. *Introductory solid state physics*. London: Taylor & Francis; 1990.
9. Seitz F. *The modern theory of solids*. New York: McGraw-Hill; 1940.
10. Wannier GH. *Elements of solid state theory*. Cambridge: Cambridge University Press; 1954.
11. Wilson AH. *The theory of metals*. Cambridge: Cambridge University Press; 1958.
12. Ziman JM. *Principles of the theory of solids*. Cambridge: Cambridge University Press; 1972.